Numerical Investigation of the Effects of Tool Geometry on Multi-Point Forming Process

Aws Khalid Ibrahim[1,*]

[1]Department of Artificial Intelligence and Robots Engineering, College of Engineering, Al-Karkh University of Science, Baghdad, Iraq

Abstract: Metal forming is an essential technique for manufacturing of lightweight components that offer enhanced energy efficiency, functionality, and sustainability. This study presents a comprehensive numerical investigation into the influence of forming tool geometry on the quality and performance of the multi-point forming (MPF) process. Finite element simulations were employed to systematically evaluate the effects of geometric tool design variables, namely, tip geometry, shank configuration, and tip structure (solid or hollow) on the predicted forming performance responses, namely, wrinkling behavior, springback displacement, and thickness variation. The numerical results show that the parabolic and elliptical tip geometries prove superior forming performance by effectively suppressing wrinkling and minimizing springback while hemispherical and spherical tips result in increased wrinkling susceptibility and higher residual elastic stresses. Moreover, the inclined shank configuration leads to higher wrinkling and springback compared to other shank configurations. Solid tip structures induce higher wrinkling levels and springback compared to hollow tips. In addition, thickness uniformity is markedly improved when smooth tool profiles such as flat-end, elliptical, and rounded hemispherical geometries are employed. In contrast, the combined use of a hemispherical tip with a square section and an inclined shank results in the most pronounced thickness variation. Furthermore, solid tip designs generally promote a more uniform thickness distribution across the blank, whereas hollow tips exhibit a greater tendency toward localized thinning. Ultimately, the optimal MPF tool configuration consists of a parabolic or elliptical tip geometry combined with a hollow tip and a straight shank configuration, as it presents the best compromise for minimizing wrinkling and springback while maintaining acceptable thickness distribution.

Keywords: Wrinkling, Springback, Thickness, Finite element simulation, Sheet metal, Multi-point forming.

1. INTRODUCTION

Recent manufacturing technologies have relied heavily on metal forming since material shaping allows for production with significantly closer resemblance to the parts final geometry than typically encountered through other processes. This capability not only lessens the cost of production, but also provides opportunities for mechanical properties tailoring that caters to global requests for advanced technologies in metalworking [1]. Sheet forming is a widely used process for numerous applications due to its ability to mass manufacture lightweight metallic components. Similar to many other processes, a die set is needed to create the sheet metal into your required shape for perfect sheet forming operation. However, the production of dies takes time and is expensive. Efforts have been made in the last years to overcome the disadvantages of conventional sheet metal forming process. A technology called multipoint forming (MPF), which is considered a flexible and advanced metal sheet component production method, was developed to increase the flexibility of the sheet-forming process via reconfigurable dies [2]. The basic idea involves arranging a set of uniformly-shaped and sized pins in an arrangement that could be pattern formation in rectangular, square or even circular formations. The desired form is then achieved by varying the heights of the pins [3]. The punch system is easy to control, which can produce surfaces of different profiles by adjusting the pin height in the lower and upper molds. This eliminates the need to design and manufacture separate dies for each part, making it possible to produce components with different geometries from a single die set. This allows minimizing lead time and production cost, especially in the case of makespan and customized manufacturing [4]. The upper and lower dies further comprise a number of separately moveable components enabling modeling of a range of surface topographies [5].

Several studies have examined sheet metal forming processes, especially multi-point forming (MPF), due to its flexibility and suitability for producing complex geometries. Wei Shen *et al.* [6] developed an approximate analytical approach for evaluating stresses in repeated forming operations and derived expressions for estimating residual stresses in curved plates. A simulation procedure was also proposed to evaluate residual stress distributions in plates formed by repeated MPF processes, and the results showed good agreement with theoretical predictions. Petra Maier *et al.* [7] studied MPF using adjustable flexible dies in which mobile punch elements replace conventional fixed dies. Forming limits and an appropriate forming algorithm were established to ensure continuous surface generation while minimizing dimpling and wrinkling. The use of a polyurethane

*Address correspondence to this author at the Department of Artificial Intelligence and Robots Engineering, College of Engineering, Al-Karkh University of Science, Baghdad, Iraq; E-mail: aws.khalid@kus.edu.iq

Received on 02-06-2026 Accepted on 17-07-2026 Published on 25-07-2026

E-ISSN: 2409-9848/26

elastic cushion was found to be effective in suppressing dimples. Experimental observations obtained from a laboratory-scale nine-point die device were used to support scaling of the forming algorithm to an MPF machine equipped with twenty-four opposing punch pairs. The study indicated that surface quality requirements, including the prevention of wrinkling, dimpling, and edge buckling, represent the main constraints of the process rather than material hardening effects.

Heli Peng *et al.* [8] introduced the MPF process applied to polycarbonate sheets by establishing a geometric relationship between the punch element and the desired surface, besides proposing a simplified scheme for calculating pin heights. Finite element simulations of saddle and spherical-shaped parts were conducted using an explicit dynamic formulation, leading to the identification of suitable process parameters. The results showed good shape accuracy, confirming the feasibility of MPF for forming polycarbonate sheets and the sensibility of the forming parameters realized by numerical simulations. Xinqi Li *et al.* [9] conducted a research on springback in MPF and classified previous works into theoretical developments, numerical investigations, and control approaches of springback. Based on this analysis, the authors suggested that future improvements in springback control may be achieved through the integration of high-frequency ultrasonic excitation techniques with artificial intelligence for compensation control of springback during the forming process. Abror Tolipov *et al.* [10] proposed an optimization study including a hole-type rubber punch designed to replace the upper pin matrix in multipoint incremental forming in order to simplify pin alignment and to minimize setup time. Finite element simulations combined with design of experiments indicated that hole size was the most significant parameter for all responses, whereas the material compression ratio was proved to have insignificant effects on shape deviation and wrinkling. Experimental validation showed a substantial improvement in wrinkling reduction of 80% compared to employing a solid rubber punch. B. Beglarzadeh *et al.* [11] studied sheet behavior in multi-point deep drawing and identified several defects associated with the forming operation. Defects generated in parts produced by the MPF process were explored and sheet rupture was predicted using ductile fracture criteria.

Furthermore, the effect of blank holder force was analyzed for polyurethane layers with different hardness levels. The results indicated that higher polyurethane hardness is accompanied with increased blank holder force, whereas thicker polyurethane layers reduce indentation rates. Xinqi Li *et al.* [12] explored the fundamental theory for the combined effects of multi-point stamping and ultrasonic vibration-assisted forming, including comparisons of material parameters during multi-point stamping technique with and without ultrasonic excitation, changes in stress–strain behavior at various frequencies, and springback characteristics under different operating conditions.

Viorel Paunoiu *et al.* [13] performed finite element simulations to evaluate the effect of interpolator behavior on part properties, with particular consideration to quality indicators, namely; stress distribution and springback. The findings provide guidance for the development of improved die design concepts. Ali Elghawail *et al.* [14] utilized a polyurethane elastic punch rubber in combination with a reconfigurable MPF die in order to minimize tooling time and cost. The results showed a substantial decrease in springback and wrinkling in the formed part even in the absence of a blank holder. Alyaa Al-Ghuraibawi *et al.* [15] conducted numerical simulations of MPF process for two configurations: the first involves a direct contact forming between sheet metal and pins while the second case is forming with an intermediate rubber layer. The findings showed that introduction of the rubber layer significantly suppressed surface dimpling and reduced the maximum strain and stress of the blank profile by approximately 49% and 27%, respectively. A A Tolipov *et al.* [16] further observed the effects of process parameters such as radius of curvature, blank holder force, elastic cushion thickness and friction coefficient on quality of parts produced by flexible multi-point stamping dies. The results confirmed that applying a variable blank holder force instead of a constant value improves forming behavior and allows more uniform deformation. Comparisons with numerical simulations for hemispherical shapes proved that the use of a polyurethane cushion reduces maximum shape deviation and suppresses sheet wrinkling.

In modern engineering applications, the finite element (FE) approach is an extensively used numerical technique adopted for processing and analyzing complex engineering problems including multi-physics interactions, heat transfer, and structural mechanics. Owing to its flexibility, this method is widely utilized in several engineering applications for predicting the structural response of various structures and materials under different loading conditions, and it is usually employed as an optimization tool for novel design features [17].

Recent studies have continued to improve the performance of multi-point forming (MPF) by addressing different aspects of the process. Majidabad *et al.* [18] optimized the forming limit of Al/Cu bimetallic sheets by investigating the effects of pin size, layer arrangement, and polyurethane properties. Yang *et al.* [19] focused on improving the numerical accuracy of flexible multi-point stretch-bending by evaluating different material constitutive models. Hao *et al.* [20] proposed a hexagonal multi-point tooling configuration to enhance the surface quality of thermoformed composite components. In addition, Ding *et al.* [21] developed a strategy based on sequential loading to suppress wrinkling in high-strength steel components during MPF.

Although these studies significantly improved process performance, they mainly emphasized process optimization, material behavior, and forming strategies rather than the systematic design of the forming tool geometry. Despite these significant advances, limited attention has been devoted to the systematic influence of forming tool geometry itself. In particular, no previous study has comprehensively evaluated the combined effects of tool tip geometry, shank configuration, and tip structure on the principal quality indicators of MPF, namely wrinkling, springback, and thickness. To address this research gap, the present study performs a comprehensive finite element investigation into the effects of forming tool geometry variables, namely tool tip geometry, (including parabolic, elliptical, flat end, spherical and hemispherical with round and square sections), shank configuration (involving inactive, inclined, and straight), and tip structure (hollow and solid) of the forming tool on key indicators of the forming quality, namely wrinkling behavior, springback displacement, and thickness variation.

Unlike previous studies, which mainly optimized process parameters or investigated isolated tooling characteristics, this work provides an integrated evaluation of forming tool geometry and identifies the optimum tool configuration for minimizing forming defects while improving deformation quality. The findings provide practical design guidelines for flexible multi-point forming tooling and contribute to a deeper understanding of the underlying tool–sheet interaction mechanisms.

2. MATERIALS AND METHODS

2.1. Geometry of Forming Tools

In this study, six types of tool tip geometry are used; which are: spherical, hemi-spherical with round and square section, flat end, elliptical, and parabolic geometry. In addition, configurations of straight, inclined, and inactive (or thin) shank are employed for each type of tool geometry. Besides, the structure of the tool tip (hollow or solid) is also considered for all tool shapes. All forming tools have been designed with a diameter of 12 mm throughout all FE models. Regarding tools with a hollow tip, the hole diameter is selected to be a half of the primary tool diameter in order to analyze its effects on MPF operation. Table **1** illustrates various geometries, shank configurations, and tip structures of the forming tools in details that are adopted in this work.

2.2. Numerical Modelling of Multi-Point Forming

Finite element (FE) simulations were accomplished using ANSYS Forming 2023 R1 to examine how tool (pin) geometry affects the multi-point forming process. The FE setup, illustrated in Figure **1**, consists of a rectangular sheet blank positioned between two opposing pin matrices. All forming tools were designed with a tip diameter of 12 mm. Detailed geometric dimensions and classifications of the different tool configurations are provided in Table **1**. Each matrix contains a 17 × 17 array of pins uniformly distributed along the X and Y directions, arranged in a face-to-face configuration. In the model, the upper and lower pin matrices represent the punch and die set, respectively. The distance of separation between adjacent pins was fixed at 0.5 mm. Interfacial contact interactions between all forming components were defined using a universal contact formulation, while a friction coefficient of μ = 0.1 was assigned at the interfaces between all parts [10]. Both punch and die assemblies (tooling set) were treated as rigid bodies in the simulations.

The sheet material selected for the analysis was DC05 steel with general dimensions of 200 mm × 200 mm × 1 mm. The intended final shape corresponds to a cylindrical surface with an inner radius of 250 mm. Mechanical properties of the DC05-steel material are summarized in Table **2**. The material behavior was assumed to be isotropic, and an elastoplastic constitutive model was adopted. The flow stress response was described using the power-law relationship given in Eq. (1) [22]:

$$\sigma = K.\varepsilon^n \quad (1)$$

where σ is the true stress (MPa), ε is the true strain (dimensionless), n is the strain-hardening exponent (dimensionless), and K represents the strength coefficient (MPa).

The blank was modeled as a deformable body and meshed using 4-node shell elements (SHELL163-type) with a uniform element size of 1 mm. This configuration results in a structured mesh of square elements with a total number of 40,000 elements across the sheet surface. In contrast, the pin matrices of the punch and die sets were meshed using rigid 3D solid elements (Tetrahedral-type).

Table 1: Various Geometries of Forming Tools that are used in the Study

No.	Tip Geometry	Tip Structure / Shank Configuration: Solid			Hollow		
		Straight	Inclined	Inactive (thin)	Straight	Inclined	Inactive
1	Spherical	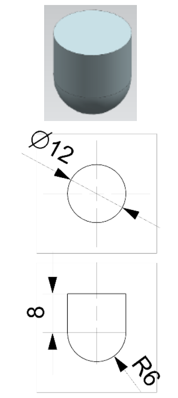	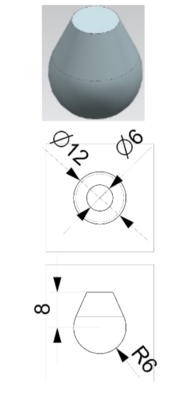	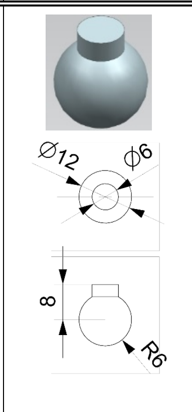	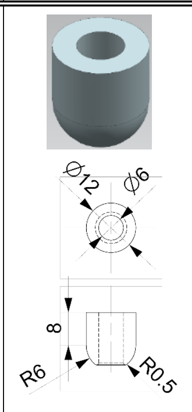	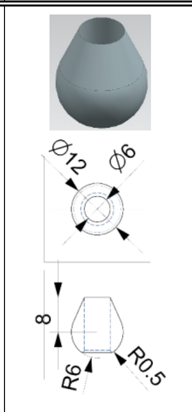	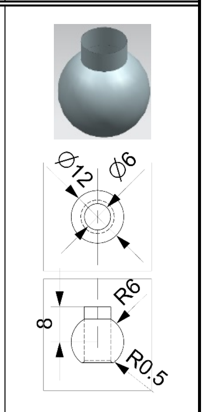
2	Hemi-spherical / Round Section	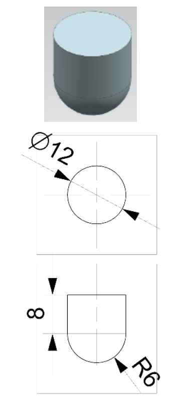	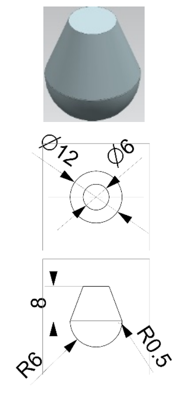	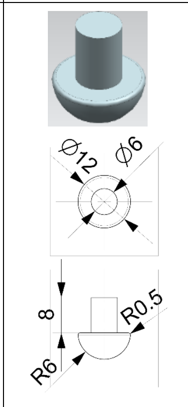	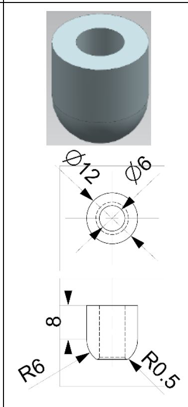	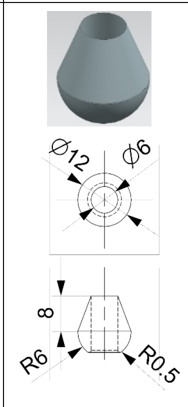	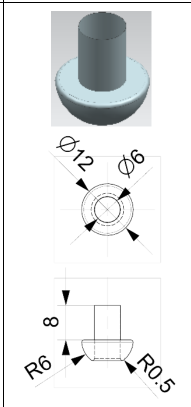
3	Hemi-spherical / Square Section	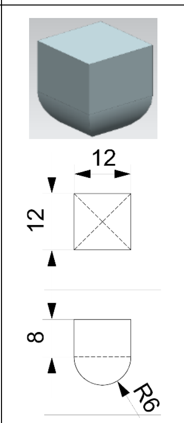	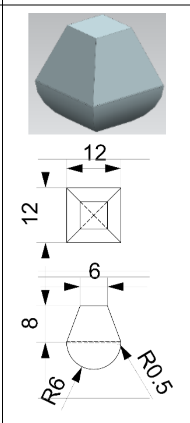	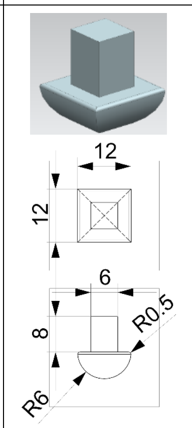	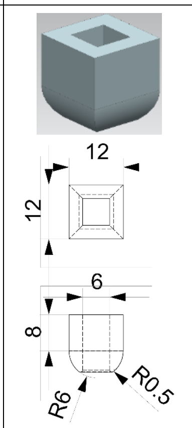	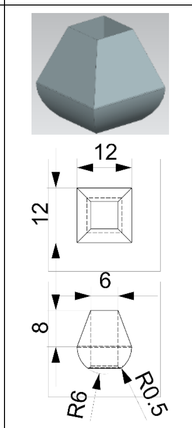	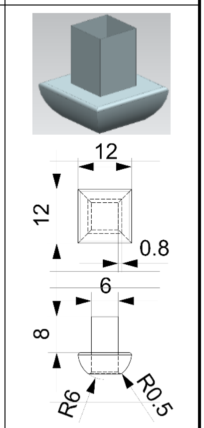
4	Flat End	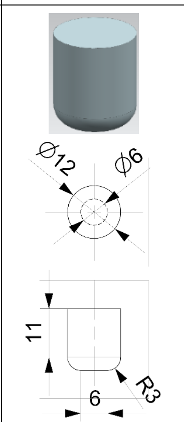	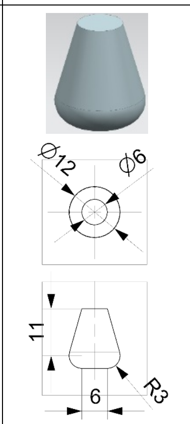	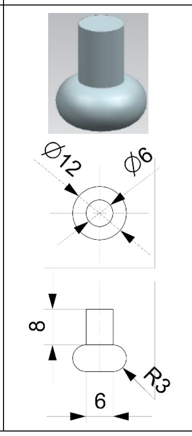	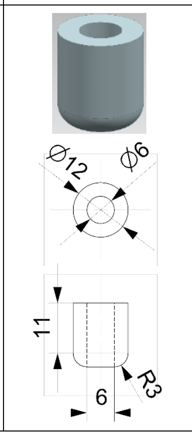	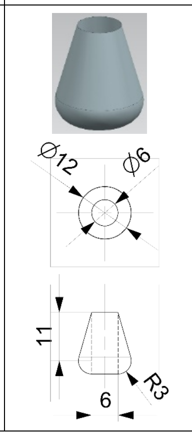	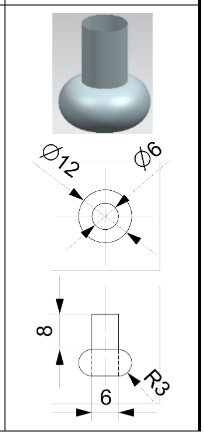

5	Elliptical	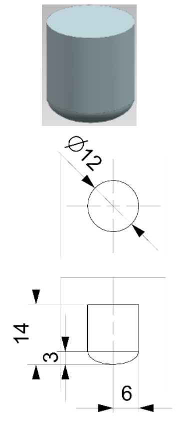	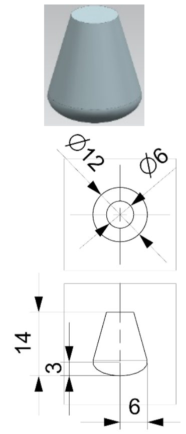	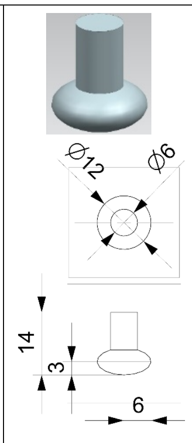	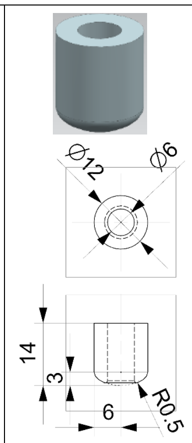	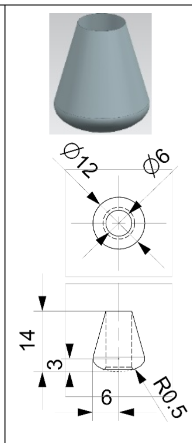	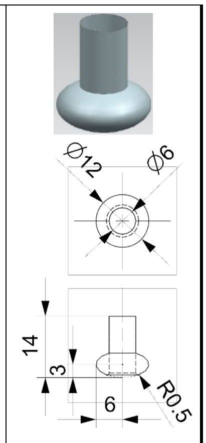
6	Parabolic	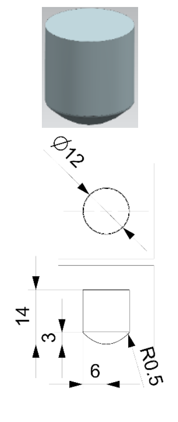	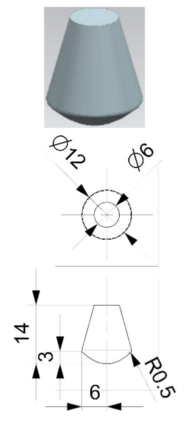	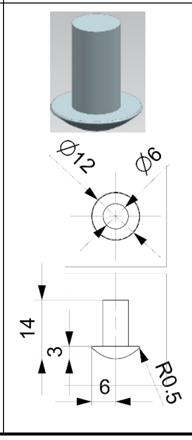	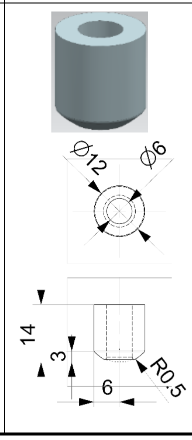	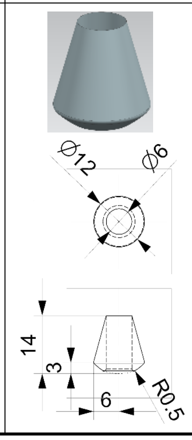	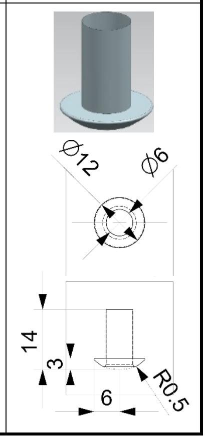

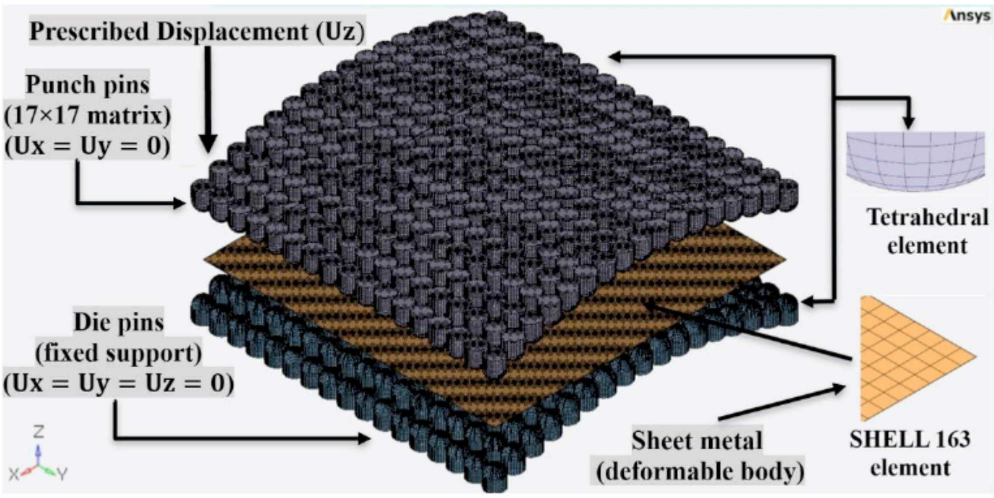

Figure 1: Sketch of the FE model with boundary conditions and element type.

Table 2: Mechanical Properties of the Sheet Material (DC05-Steel)

Category	Quantity
Elastic modulus	220 GPa
Yield stress	201.9 MPa
Poisson ratio	0.3
Strain-hardening exponent	0.17
Strength coefficient	527.13 MPa
Density	7870 Kg/m3

Appropriate displacement boundary conditions were applied to represent the forming operation. Accordingly, the die pins were fixed in all translational directions (X, Y, and Z) in order to act as a rigid supporting surface, while the sheet metal was allowed to deform freely through the defined contact interactions with the punch and die. The punch pins were restricted in the X and Y directions for preventing lateral movement, while forming was achieved by applying a prescribed punch displacement along the Z-axis (as shown in Figure **1**), considering both the initial sheet thickness and the maximum forming depth required for realizing the final geometry. It is important to highlight that the forming load was not directly defined as an input parameter; instead, it was considered as a reaction force developed as a result of the punch displacement and the contact interactions between the punch, sheet, and die throughout the forming operation.

An explicit solution scheme available in ANSYS Forming 2023 R1 was employed to handle the highly nonlinear contact interactions and to avoid convergence problems associated with the large number of elements and model complexity. Double precision calculations were enabled throughout all FE simulations in order to minimize round-off errors. No elastic cushion was introduced in the current models in order to obtain a single-curvature surface that closely matches or -at least- approaching the intended geometry. Furthermore, a blank holder was not included, allowing the sheet edges to deform freely during the forming operation [23].

2.3. Mesh Convergence and Numerical Accuracy

To evaluate the influence of mesh density on the numerical predictions and to ensure the reliability of the finite element simulations, a mesh convergence study was conducted using a representative forming case (Run 1). Three different element sizes, namely 1.5 mm, 1.0 mm, and 0.5 mm, were investigated while maintaining identical material properties, boundary conditions, contact definitions, and process parameters. The corresponding numerical predictions for wrinkling, springback displacement, and thickness variation are summarized in Table **3**.

It can be observed that refining the mesh from 1.5 mm to 1.0 mm resulted in noticeable changes in all evaluated responses, indicating that the coarse mesh was insufficient to accurately capture the deformation characteristics. In contrast, further refinement from 1.0 mm to 0.5 mm produced only relatively small differences, with variations of 5.34%, 3.57%, and 3.40% for wrinkling, springback displacement, and thickness variation, respectively, as summarized in Table **4**. These limited differences indicate that the numerical predictions gradually approach mesh-independent solutions as the mesh becomes finer.

Although the 0.5 mm mesh provides slightly higher numerical accuracy, it requires substantially greater computational time and memory consumption. Therefore, the 1.0 mm mesh was selected for all subsequent simulations because it provides a satisfactory compromise between computational efficiency and numerical accuracy while maintaining reliable prediction of the investigated forming responses.

2.4. Model Validation

In order to verify the robustness of the proposed FE model, a validation procedure was considered by comparing the results of FE simulation with the experimentally published data retrieved from the study conducted by Moheen *et al*. [24]. As mentioned earlier; for the purpose of analysis, neither blank holder nor elastic cushions are included in the developed FE model leading to a delayed deformation and then a sudden increase in the punch load (as depicted in Figure **2**) contrary to the experimental study where elastic cushion is adopted. However, similar forming parameters, geometrical conditions, and material properties reported in the experimental study were used to reconstruct the FE model and to ensure a consistent comparison between the numerical and experimental results. Accordingly, the general trend or behavior of the forming force is largely similar for both simulation and experimental results.

Table 3: Mesh Convergence Study for the Representative Forming Case (Run 1)

Mesh size (mm)	Wrinkling (mm)	Springback Displacement (mm)	Thickness Variation (mm)
1.5	0.325701	0.238661	0.0420581
1.0	0.273776	0.210843	0.0371317
0.5	0.259150	0.203310	0.0358691

Table 4: Percentage Difference between Successive Mesh Sizes

Comparison	Wrinkling (%)	Springback (%)	Thickness variation (%)
1.5 - 1.0 mm	15.95	11.66	11.71
1.0 - 0.5 mm	5.34	3.57	3.40

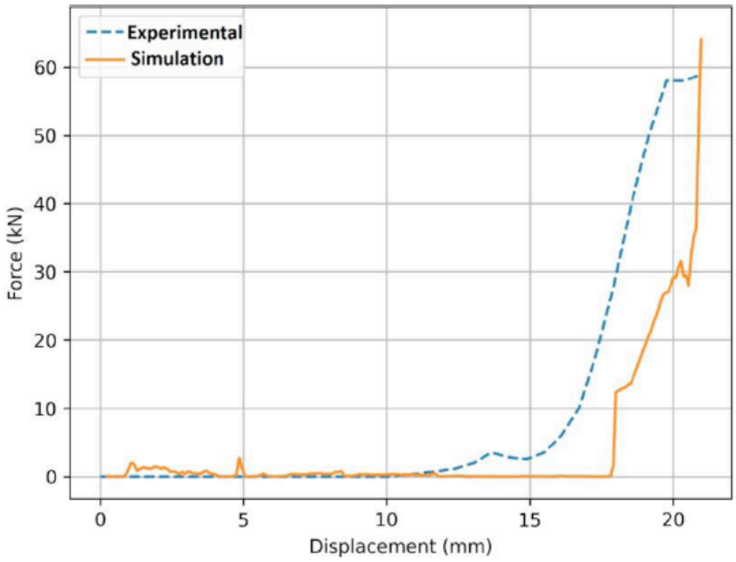

Figure 2: Force-displacement curves of the simulation and experimental results.

Figure **2** also shows that the rise in force is up to 12 KN which corresponds to a punch displacement of about 18 mm where the pins are in contact with the surface of the sheet indicating the onset of plastic deformation. After that point, a relatively gradual rise in force to about 30 KN followed by a rapid increase until the end of punch stroke owing to strain hardening of the sheet material. The maximum predicted load by the FE model was 65.1 KN compared with 58.9 KN obtained from the experimental data that are recorded by Moheen *et al*. [24]. This results in a maximum discrepancy of about 10 % between the simulation and experimental results.

Overall, the comparison demonstrates a satisfactory agreement between the numerical predictions and the available experimental data, particularly with respect to the overall force–displacement response and the maximum forming load. The observed discrepancy can be attributed to the simplifying assumptions adopted in the finite element model, including the exclusion of the blank holder and elastic cushion, as well as the inherent uncertainties associated with material properties, contact conditions, and experimental measurements. Nevertheless, the relatively small difference in the predicted maximum load and the close agreement in the overall deformation behavior confirm that the developed FE model is capable of reliably capturing the mechanical response of the multi-point forming process. Therefore, the validated numerical model provides a reliable basis for investigating the influence of the selected tool geometry parameters on wrinkling, springback displacement, and thickness variation in the subsequent analyses.

2.5. Process Variables and Performance Indicators

The main process variables were selected as tip geometry, shank configuration, and tip structure of the forming tool whereas wrinkling, springback displacement, and thickness variation were considered as the response indicators to represent the quality of parts shaped by MPF. The simulation cases were generated based on a full factorial combination of the examined tool geometry variables. Such approach ensures that all possible combinations of the selected variables and their levels were taken into consideration in order to evaluate their effects on the forming responses (performance indicators) predicted by the FE model. As all variables introduced are of categorial quantities, thus it is worth to manipulate their levels by coding approach for the purpose of constructing the simulation set and conducting the analysis for the process variables. The method of coding the levels of tool tip geometry were considered depending on the larger size of the active curvature tip contributing to forming process while the hemispherical tip with a square section was coded to the higher level as its square perimeter circumscribes a circle of 12 mm diameter. Regarding the levels of shank configuration and structure of tool tip variables, they are coded depending on their larger contact area contributing to the forming operation. The full factorial combination method was used to generate a set of simulation runs for three process variables in which each factor varies over different level ranges from the lowest to the highest value. Table **5** shows the process variables with their levels and codes utilized in this work.

In addition, it is important to highlight that all other technological parameters (*i.e*. tool speed, punch stroke,

Table 5: Process Variables with Levels

Variable	Level / (Code)					
Tip Geometry	Parabolic (1)	Elliptical (2)	Flat end (3)	Hemispherical-round section (4)	Spherical (5)	Hemispherical-square section (6)
Shank Configuration	Inactive (1)		Inclined (2)		Straight (3)	
Tip Structure	Hollow (1)			Solid (2)		

etc.) were kept constant during all simulation cases in order to eliminate their influence and particularly assess the effects of tool geometry variables on the forming performance. Although parameters such as the friction coefficient, pin spacing, sheet material properties, boundary conditions, and loading conditions may influence the absolute values of wrinkling, springback displacement, and thickness variation by affecting the contact conditions and material flow during the forming process, maintaining identical process conditions for all simulation cases ensured that the observed differences in the numerical predictions could be attributed primarily to the investigated tool geometry variables. Consequently, the adopted modelling strategy provided a consistent and reliable basis for the comparative assessment of the effects of tool geometry on the forming performance.

With respect to the evaluated process responses or performance indicators, wrinkling was quantified by measuring the normal distance between the formed geometry and the reference CAD model at each wrinkle peak. The magnitude of the overall wrinkling was expressed using the root-mean-square error (RMSE), as given in Eq. (2) [22]. Springback defines the elastic recovery that occurs after the instant removal of the applied bending load, causing a partial return of the metal toward its original configuration [25]. In this study, springback was characterized by calculating the RMSE of the absolute displacements resulting from unloading, and can be calculated according to Eq. (3). In addition, sheet thickness was recorded at multiple zones across the formed part to determine spatial variation. Rather than reporting individual measurements, thickness uniformity was evaluated through the standard deviation of the dataset, defined here as the thickness variation, and can be computed using Eq. (4) [24].

$$W_r = \sqrt{\frac{1}{n}\sum_{i=1}^{n} Uz_i^2} \quad (2)$$

where W_r is the wrinkling indicator (mm), *Uzi* denotes the amplitude of an individual wrinkle (mm) and n represents the total number of wrinkling waves considered.

$$S = \sqrt{\frac{1}{n}\sum_{i=1}^{n} d_i^2} \quad (3)$$

where S is the springback displacement (mm), d_i corresponds to the absolute-normal displacement after unloading (mm), and n is the total number of measured points.

$$t = \sqrt{\frac{1}{N}\sum_{i=1}^{N} (x_i - \bar{x})^2} \quad (4)$$

where t is the thickness variation (mm), x_i denotes an individual thickness measurement (mm), $\bar{x}$ is the mean thickness of all recorded values (mm), and N represents the total number of measurement points.

3. RESULTS AND DISCUSSION

Table **6** shows the generated plan of 36 simulation runs based upon a full-factorial combination and the evaluated performance indicators (responses). The entire 36 FE models are presented in the Appendix.

3.1. Wrinkling

Wrinkling represents one of the most critical instability modes in sheet metal forming, as it compromises both geometric accuracy and surface finish of the formed component. The numerical findings obtained in this study indicate that wrinkle development in the MPF process is not governed by a single variable, but rather by the combined effects of tip geometry, shank configuration, and tip structure of the forming tool, as illustrated in Figure **3**. Figure **4** shows FE simulation of wrinkling formation through MPF process adopted in this study.

The FE simulations reveal an obvious variation in wrinkle severity among the studied tool tip geometries. In particular, the parabolic and elliptical tip geometries prove a noticeably improved ability to suppress wrinkling compared to flat-end, hemispherical, and spherical tips. This behavior can be interpreted in terms of contact mechanics. The smoother tool profile associated with the elliptical and parabolic tips promotes a more uniform distribution of contact pressure over the sheet surface. As a result, localized

Table 6: Simulation Results for, Wrinkling, Springback Displacement, and Thickness Variation

Run No.	Process Variables (Factors)						Responses		
	Tip Geometry		Shank Configuration		Tip Structure		Wrinkling (mm)	Springback Displacement (mm)	Thickness Variation (mm)
	Uncoded	Coded	Uncoded	Coded	Uncoded	Coded			
1	Parabolic	1	Inactive	1	Hollow	1	0.273776	0.210843	0.0371317
2	Parabolic	1	Inclined	2	Solid	2	1.444010	1.541947	0.00495622
3	Parabolic	1	Straight	3	Hollow	1	0.250755	0.259128	0.0343282
4	Parabolic	1	Inactive	1	Solid	2	0.717230	0.791258	0.00460264
5	Parabolic	1	Inclined	2	Hollow	1	0.857378	0.920895	0.06468583
6	Parabolic	1	Straight	3	Solid	2	0.730691	0.801111	0.00460838
7	Elliptical	2	Inactive	1	Hollow	1	0.542743	0.567976	0.05678014
8	Elliptical	2	Inclined	2	Solid	2	0.658409	0.701075	0.01019406
9	Elliptical	2	Straight	3	Hollow	1	0.514634	0.533283	0.046359
10	Elliptical	2	Inactive	1	Solid	2	0.227802	0.254935	0.01210868
11	Elliptical	2	Inclined	2	Hollow	1	0.501468	0.522598	0.04269074
12	Elliptical	2	Straight	3	Solid	2	0.624999	0.685277	0.01347995
13	Flat End	3	Inactive	1	Hollow	1	0.533872	0.585043	0.02952706
14	Flat End	3	Inclined	2	Solid	2	1.570249	1.703469	0.02835127
15	Flat End	3	Straight	3	Hollow	1	0.535121	0.58593	0.02951268
16	Flat End	3	Inactive	1	Solid	2	1.288997	1.394673	0.02929707
17	Flat End	3	Inclined	2	Hollow	1	0.958996	1.03096	0.0417093
18	Flat End	3	Straight	3	Solid	2	1.327546	1.434904	0.02936894
19	Hemi-spherical Round	4	Inactive	1	Hollow	1	0.35777	0.39585	0.02631303
20	Hemi-spherical Round	4	Inclined	2	Solid	2	1.788251	1.909795	0.00727323
21	Hemi-spherical Round	4	Straight	3	Hollow	1	0.901741	0.981247	0.03118869
22	Hemi-spherical Round	4	Inactive	1	Solid	2	1.79053	1.927432	0.02106366
23	Hemi-spherical Round	4	Inclined	2	Hollow	1	0.792641	0.870077	0.02715535
24	Hemi-spherical Round	4	Straight	3	Solid	2	1.68495	1.783307	0.00396732
25	Spherical	5	Inactive	1	Hollow	1	0.775525	0.856044	0.02682475
26	Spherical	5	Inclined	2	Solid	2	1.55941	1.672292	0.00897803
27	Spherical	5	Straight	3	Hollow	1	0.901741	0.981247	0.03118869
28	Spherical	5	Inactive	1	Solid	2	1.460686	1.566541	0.00541618
29	Spherical	5	Inclined	2	Hollow	1	0.926574	1.016487	0.02786255
30	Spherical	5	Straight	3	Solid	2	1.68495	1.783307	0.00396732
31	Hemi-spherical Square	6	Inactive	1	Hollow	1	0.49847	0.55104	0.10859836
32	Hemi-spherical Square	6	Inclined	2	Solid	2	1.181319	1.249801	0.00501946
33	Hemi-spherical Square	6	Straight	3	Hollow	1	0.776801	0.831871	0.16139977
34	Hemi-spherical Square	6	Inactive	1	Solid	2	0.816941	0.88024	0.00405069
35	Hemi-spherical Square	6	Inclined	2	Hollow	1	0.96112	1.060195	0.20127897
36	Hemi-spherical Square	6	Straight	3	Solid	2	0.52468	0.582395	0.00497635

in-plane compressive stresses-primarily responsible for wrinkling-are alleviated.

From a mechanical perspective, wrinkling in MPF arises from the accumulation of excessive compressive stresses that develop during localized deformation. By

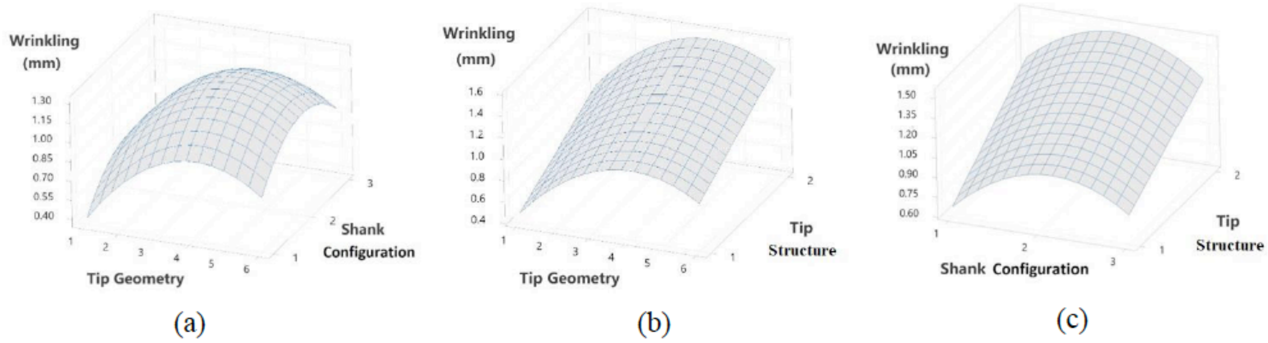

Figure 3: Effect of forming tool variables on wrinkling.

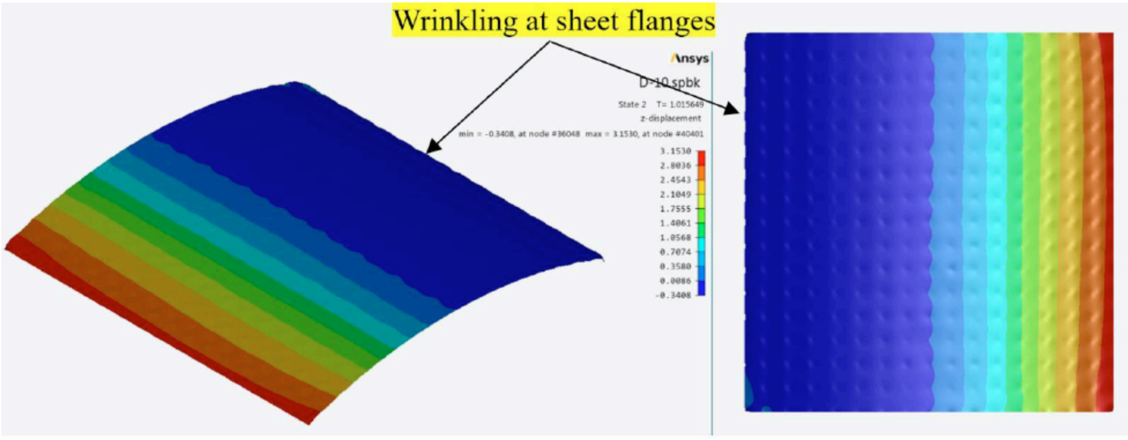

Figure 4: FE simulation of wrinkling formation at sheet flanges.

mitigating stress concentrations at the tool–sheet interface, these smoother geometries effectively delay the onset of instability and thus the initiation of wrinkling. In contrast, hemispherical and spherical tips tend to concentrate loads over smaller contact regions, especially under non-uniform loading conditions, thereby intensifying local compressive stresses and increasing wrinkling susceptibility. This finding is consistent with previously reported observations on MPF and incremental forming studies, which reported that distributions of non-uniform contact pressure and concentrations of localized compressive stresses were identified as principal contributors to wrinkle initiation (Jeswiet *et al.* [26]; Cai *et al.* [27]).

More broadly, increasing the smoothness of the effective contact area at the tool-sheet interface enhances forming stability by distributing deformation over a wider zone, which delays membrane instability and thus reduces wrinkling. The current study further introduces that even small variations in tool curvature can produce measurable differences in wrinkle magnitude, highlighting the sensitivity of MPF to geometric tool design.

Furthermore, the superior wrinkling resistance exhibited by the parabolic and elliptical tool geometries can also be explained by their influence on the evolution of the stress–strain field during deformation. The smoother contact profile promotes a gradual transition from elastic to plastic deformation, allowing plastic strains to develop more uniformly over a wider deformation zone. Consequently, stress redistribution becomes more homogeneous, reducing steep strain gradients and localized compressive bands that act as precursors to buckling instability. In contrast, hemispherical and spherical tool geometries tend to induce highly localized plastic deformation accompanied by pronounced stress concentrations, thereby accelerating the onset of local instability and wrinkle formation. These observations indicate that the effectiveness of tool geometry is governed not only by the distribution of contact pressure but also by its ability to control stress redistribution, plastic strain evolution, and deformation stability throughout the MPF process, which is consistent with recent investigations on optimized multi-point forming tooling and forming strategies (Majidabad *et al.* [18]; Hao *et al.* [20]; Ding *et al.* [21])

On the other hand, Although the effect of shank configuration on wrinkling is statistically insignificant, but its effect remains evident. As shown in Figure **3**, the inclined shank configuration consistently produces higher wrinkle amplitudes than the straight or inactive shanks. This can be attributed to the non-uniform force transmission mechanism combined with asymmetric loading conditions associated with the inclined shank, which generates non-uniform deformation patterns and increases compressive stress gradients and thus promotes instability in the sheet leading to accelerate wrinkling in flexible forming systems (*i.e.* MPF). Furthermore, the inclined shank also introduces additional bending and shear effects, disturbing the internal stress equilibrium within the blank and thus facilitating favorable conditions for wrinkle initiation and growth. The present numerical results quantitatively confirm these observations within the MPF framework. In contrast, the straight and inactive shank configurations maintain a more stable and symmetric load transmission path, reducing compressive stress gradients and thus improving resistance to wrinkling. These findings align with classical thin-sheet instability theory, where non-uniform or eccentric loading conditions tend to intensify compressive instability and consequently accelerate the onset of wrinkling.

In addition, the structure of the tool tip (solid vs. hollow) also exerts a noticeable effect on wrinkling behavior. The numerical results prove that tools equipped with solid tip configurations generally exhibit higher wrinkling severity compared to hollow tip designs as indicated in Figure **3**. The higher local stiffness of the solid configuration restricts material flow beneath the contact zone, encouraging the accumulation of larger compressive stresses. Conversely, hollow tool designs introduce more compliant contact conditions that facilitates gradual material redistribution and reduces stress buildup, thereby delaying wrinkle initiation. The current study further shows that the interaction effect between tool tip geometry and tip structure becomes more pronounced in terms of wrinkling behavior, suggesting a coupling mechanism that has received limited attention in earlier MPF investigations.

3.2. Springback Displacement

Springback displacement reflects the elastic recovery that occurs once the forming load is removed, and it remains one of the principal contributors to dimensional deviation in sheet metal forming. The numerical analysis performed in this study indicates that springback is strongly influenced by the geometric features of the forming tool, as illustrated in Figure **5**. A representative finite element simulation of springback developed in the formed part shaped by MPF is presented in Figure **6**.

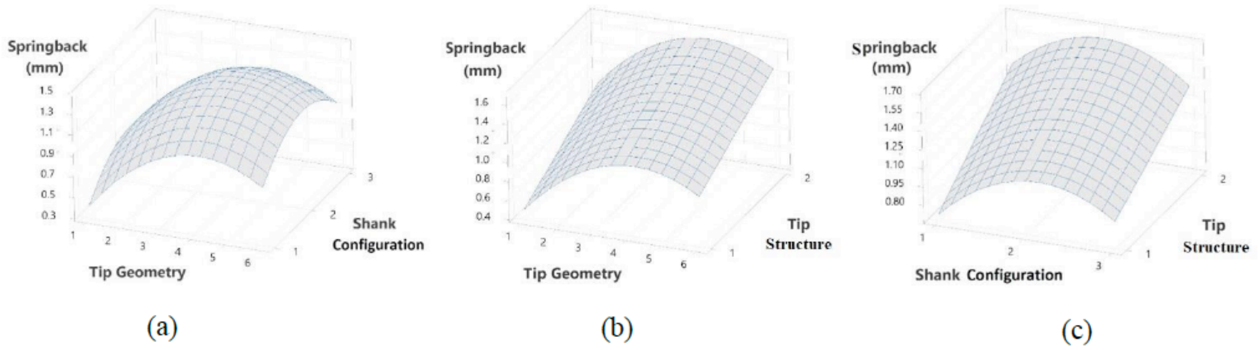

Figure 5: Effect of forming tool variables on springback displacement.

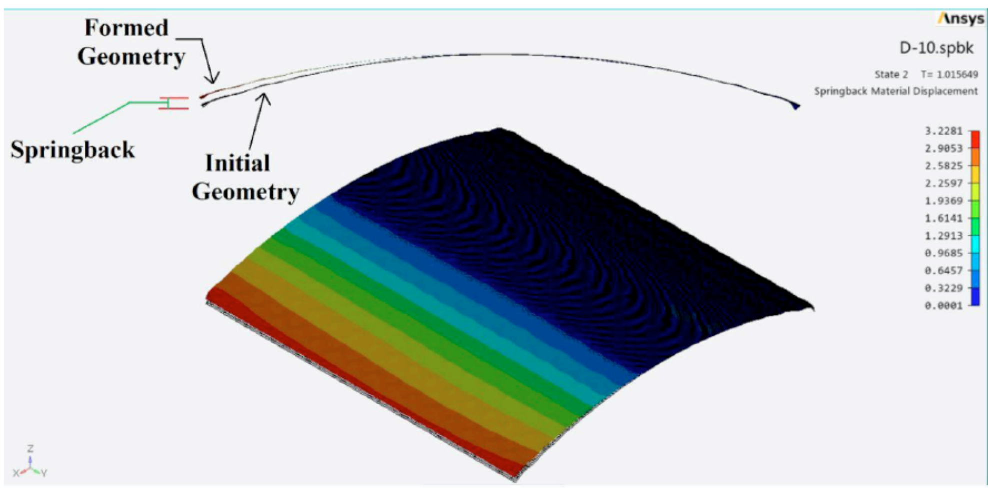

Figure 6: FE simulation of springback development in MPF operation.

The mechanical effect of shank configuration on springback is clearly noticeable. Among the investigated configurations, the inclined shank produces the largest elastic recovery, whereas the straight and inactive modes result in comparatively lower springback values (Figure **5**). This behavior can be interpreted in terms of elastic strain energy storage during deformation. The inclined shank induces non-linear stress paths within the sheet and introduces additional bending and torsional components into the deformation process, which increase the amount of recoverable elastic strain energy accumulated during forming. When the external load is released, this stored energy is partially recovered, leading to greater geometric deviation and thus larger springback displacements.

These findings are consistent with established springback theories and prior numerical investigations, which highlight that improved uniformity of plastic strain tends to reduce elastic recovery (Wagoner and Lim) [28]. Furthermore, the inclined shank configuration introduces asymmetric loading conditions, resulting in complex stress paths and higher residual elastic stresses. Since springback magnitude is primarily governed by residual stress state and stress path complexity, such asymmetry naturally intensifies the recovery effect and hence increase springback. The present results confirm these mechanisms in MPF and clearly associate increased springback with elastic energy accumulation induced by shank inclination.

In addition to shank configuration, tool tip geometry and tip structure play a decisive role. The simulations reveal that tools combining parabolic or elliptical tip profiles with a hollow tip structure consistently achieve the lowest springback values. This combination promotes smoother stress redistribution throughout the deformation zone and limits the development of peak residual elastic stresses in the formed blank. In contrast, hemispherical or spherical geometries coupled with solid tip structures tend to concentrate localized stresses near the contact region, thereby increasing residual elastic stresses and subsequent recovery. Similar observations have been reported in earlier studies. For instance, Ambrogio *et al.* [29] showed that improved tool–sheet contact conditions reduce force concentrations and enhance deformation stability, leading to enhanced forming accuracy, while Wagoner and Lim [28] presented that increased uniformity of plastic deformation is associated with reduced elastic recovery. More recently, Wen *et al.* [30] confirmed through combined finite element simulations and experimental investigations that effective springback control is primarily governed by the evolution of stress distribution and residual stresses during unloading. These findings are in good agreement with the present numerical results, where optimized tool tip geometries and hollow tip structures promote more uniform stress redistribution, reduce residual elastic stresses, and consequently minimize springback displacement. Collectively, these findings demonstrate that effective springback control in MPF operations can be achieved through careful optimization of tool geometry and contact conditions to regulate residual stress development and elastic energy release.

3.3. Thickness Variation

Thickness variation is widely considered as a crucial quality indicator of deformation homogeneity and structural integrity in multi-point forming (MPF). Excessive thinning not only reduces local stiffness but may also decrease load-carrying capacity and accelerate failure initiation. The interaction effects between pairs of tool variables on thickness distribution are presented in Figure **7**, while Figure **8** shows the FE simulation of thickness displaying thinning and thickening regions over the surface of the formed part.

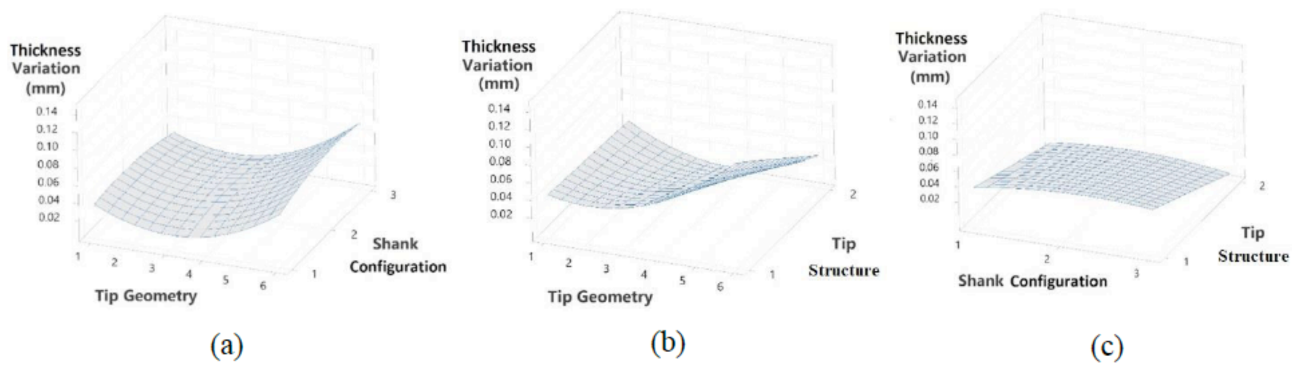

Figure 7: Effect of forming tool variables on thickness variation.

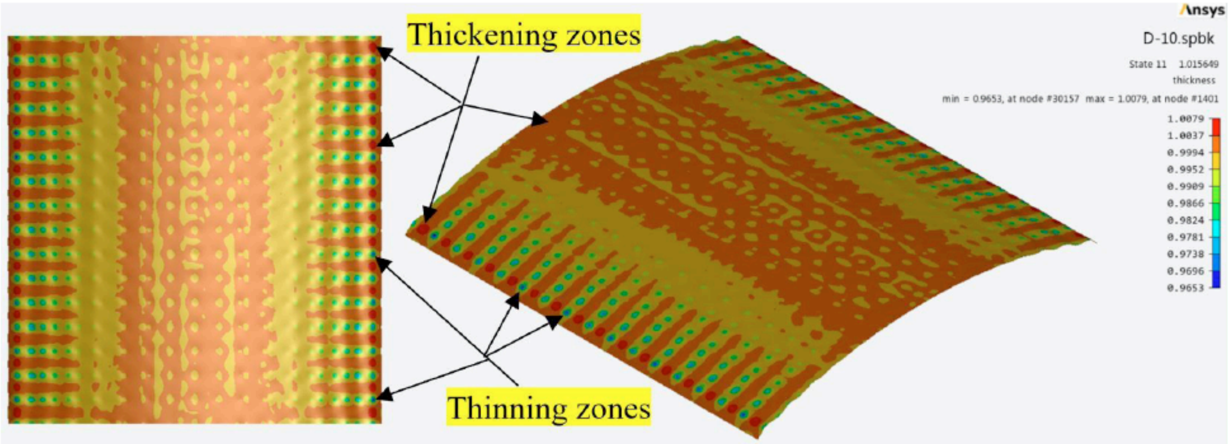

Figure 8: FE simulation of thickness in MPF process.

The simulation results clearly identify that tool tip structure as the dominant factor affecting thickness variation. As illustrated in Figure **7**, solid-tip configurations tend to maintain a more uniform thickness distribution over the blank. In contrast, hollow tips are associated with localized thinning zones. This difference can be explained by contact mechanics considerations. The solid tip presents a stiffer and more stable tool–sheet interface by maintaining a broader and mechanically stable contact zone enabling deformation to spread more uniformly throughout the forming region leading to limit excessive strain concentration, thus thickness reduction is distributed more evenly beneath the tool. A comparable mechanism was reported by Zhao and Ou [31], who demonstrated that maintaining continuous tool support and more uniform strain distribution during flexible multi-point incremental sheet forming significantly reduced sheet thinning and promoted a more uniform thickness distribution throughout the formed part.

The hollow tip, however, exhibits reduced contact stiffness, thus restricting uniform plastic strain distribution and consequently encouraging localized thinning, which intensifies thickness gradients. Comparable studies have been discussed in flexible forming research highlighting the importance of tool–sheet interaction and contact conditions in deformation stability (Allwood *et al.*) [32]. The current study quantitatively confirms this mechanism for MPF.

Tool tip geometry further contributes to thickness uniformity. In general, the flat end, elliptical, and rounded hemispherical tips generally improve thickness uniformity as smooth tool profiles reduce severe strain localization directly beneath the contact area. Previous experimental and numerical studies on incremental forming have similarly reported that gradual tool–sheet contact enhances uniform deformation and improves overall formability (Jeswiet *et al.* [26]; Ambrogio *et al.* [29]). Conversely, the combination of a hemispherical tip with a square section and an inclined shank configuration (Figure **7**) produces the most pronounced thinning. In this case, restricted material flow and intensified shear deformation beneath the tool lead to localized strain accumulation, which amplifies thickness reduction. Similar observations were reported by Cai *et al.* [27], who proved that tool configuration and non-uniform loading conditions significantly affect deformation uniformity and forming quality in multi-point forming. Overall, these findings highlight that thickness variation in MPF is governed not only by individual geometric features of the forming tool but also by their interaction. Configurations that appear acceptable when considered independently may lead to substantial thinning when unfavorable combinations of tool variables are adopted, emphasizing the necessity of integrated tool design optimization to ensure deformation stability and forming quality.

3.4. Engineering Implications of Forming Tool Configurations

The findings of the present study provide practical engineering guidelines for the design and selection of forming tools in multi-point forming (MPF) applications. The numerical results demonstrate that careful selection of tool geometry can substantially improve forming quality by reducing wrinkling and springback while maintaining acceptable thickness uniformity. In particular, parabolic and elliptical tip geometries combined with a straight shank configuration and an appropriate tip structure improves overall performance by promoting more stable material deformation and minimizing stress concentrations during the forming process. These characteristics contribute to shorter tooling preparation times, improved dimensional accuracy and reduced forming defects, thereby decreasing the need for post-forming correction and enhancing process reliability.

From an industrial perspective, the identified tool configurations can assist engineers in designing more efficient reconfigurable forming systems without requiring dedicated dies for each product geometry. This capability is particularly valuable for flexible manufacturing environments, rapid prototyping, customized production, and low-volume manufacturing, where tooling adaptability and production efficiency are of primary importance. Furthermore, minimizing wrinkling, springback, and excessive thickness variation can reduce material waste, improve product quality, and lower manufacturing costs by decreasing rework and dimensional correction operations. Therefore, the present findings provide useful engineering guidance for the design of reconfigurable tooling systems and the selection of appropriate tool configurations to improve the performance of flexible sheet metal forming systems across a wide range of industrial applications.

Although the present finite element model provides reliable comparative predictions for evaluating the influence of tool geometry on multi-point forming performance, certain limitations should be acknowledged. The present investigation is based on numerical simulations conducted under the selected material properties, tooling configurations, and process conditions considered in this study. Consequently, the reported findings should be interpreted within the scope of these conditions. Future work should include dedicated experimental validation of the most promising tool configurations, particularly those incorporating parabolic and elliptical tip geometries, to further confirm the numerical predictions under practical manufacturing conditions. In addition, extending the proposed methodology to different sheet materials, part geometries, and industrial forming scenarios would further demonstrate the applicability and robustness of the proposed approach.

4. CONCLUSIONS

The current study presents a comprehensive numerical investigation into the influence of forming tool geometry variables on the quality and performance of the multi-point forming (MPF) process. The effects of tip geometry, shank configuration, and tip structure on wrinkling behavior, springback displacement, and thickness variation were analyzed in detail using finite element simulations. The numerical results show that the parabolic and elliptical tip geometries demonstrate superior performance in suppressing wrinkling and reducing springback. This improvement is attributed to a more uniform contact pressure distribution, which mitigates in-plane compressive stress concentrations and enhances stress redistribution within the blank. In contrast, hemispherical and spherical tip geometries promote localized stress intensification under non-uniform loading conditions, leading to increased wrinkling susceptibility and higher residual elastic stresses, and consequently larger springback displacements.

In addition, the inclined shank configuration consistently results in higher wrinkling and springback compared to straight and inactive shank designs. This behavior is associated with asymmetric force transmission, non-linear stress paths, and additional bending introduced during deformation. Furthermore, solid tip configurations generally induce higher wrinkling levels and larger springback displacements than hollow tips due to their higher local stiffness, which restricts material flow and promotes compressive stress accumulation and residual stress development after unloading. Moreover, thickness uniformity is enhanced when using smooth tool profiles, such as flat-end, elliptical, and rounded hemispherical geometries, as they reduce strain localization. Conversely, the combination of a hemispherical tip with a square section and an inclined shank leads to the most severe thickness variation owing to restricted material flow and intensified shear deformation. Additionally, the solid tip configurations generally produce a more uniform thickness distribution across the blank because their wider tool-sheet interface zone promotes a more uniform plastic strain distribution, whereas the hollow tip structure tends to promote localized thinning.

In general, the optimum forming performance, characterized by reduced wrinkling and springback while maintaining satisfactory thickness homogeneity, is achieved through appropriate selection of tool geometry variables, mainly tip geometry and tip structure, highlighting their critical role in MPF tool design. In particular, forming tools incorporating parabolic or elliptical tip geometries combined with hollow tip structures provide the most favorable balance between wrinkling suppression, springback reduction, and acceptable thickness uniformity, making them promising design candidates for multi-point forming applications.

From an engineering perspective, the present findings provide practical engineering guidelines for the design of reconfigurable tooling systems used in MPF.

Careful selection of tool geometric variables can significantly improve forming quality, thereby minimizing the need for post-forming corrective operations and improving manufacturing efficiency. From a scientific perspective, the study also advances the understanding of the underlying tool–sheet interaction mechanisms and clarifies how these interactions govern elasto-plastic deformation behavior within flexible forming environments.

Future research may further extend this work by investigating additional tooling and process parameters, including frictional conditions at the tool–sheet interface, pin spacing, and blank holder conditions. Moreover, applying the proposed methodology to advanced sheet materials and more complex three-dimensional geometries would provide further insight into the broader applicability of the MPF process. Furthermore, integrating advanced optimization techniques and data-driven design approaches may contribute to further improvements in tooling design and process performance for future flexible sheet metal forming applications.

AUTHOR'S CONTRIBUTION STATEMENT

The author is responsible for all aspects of the study, including conceptualization, methodology, data acquisition, analysis, and manuscript preparation.

CONFLICTS OF INTEREST

The author declares no conflicts of interest.

APPENDIX

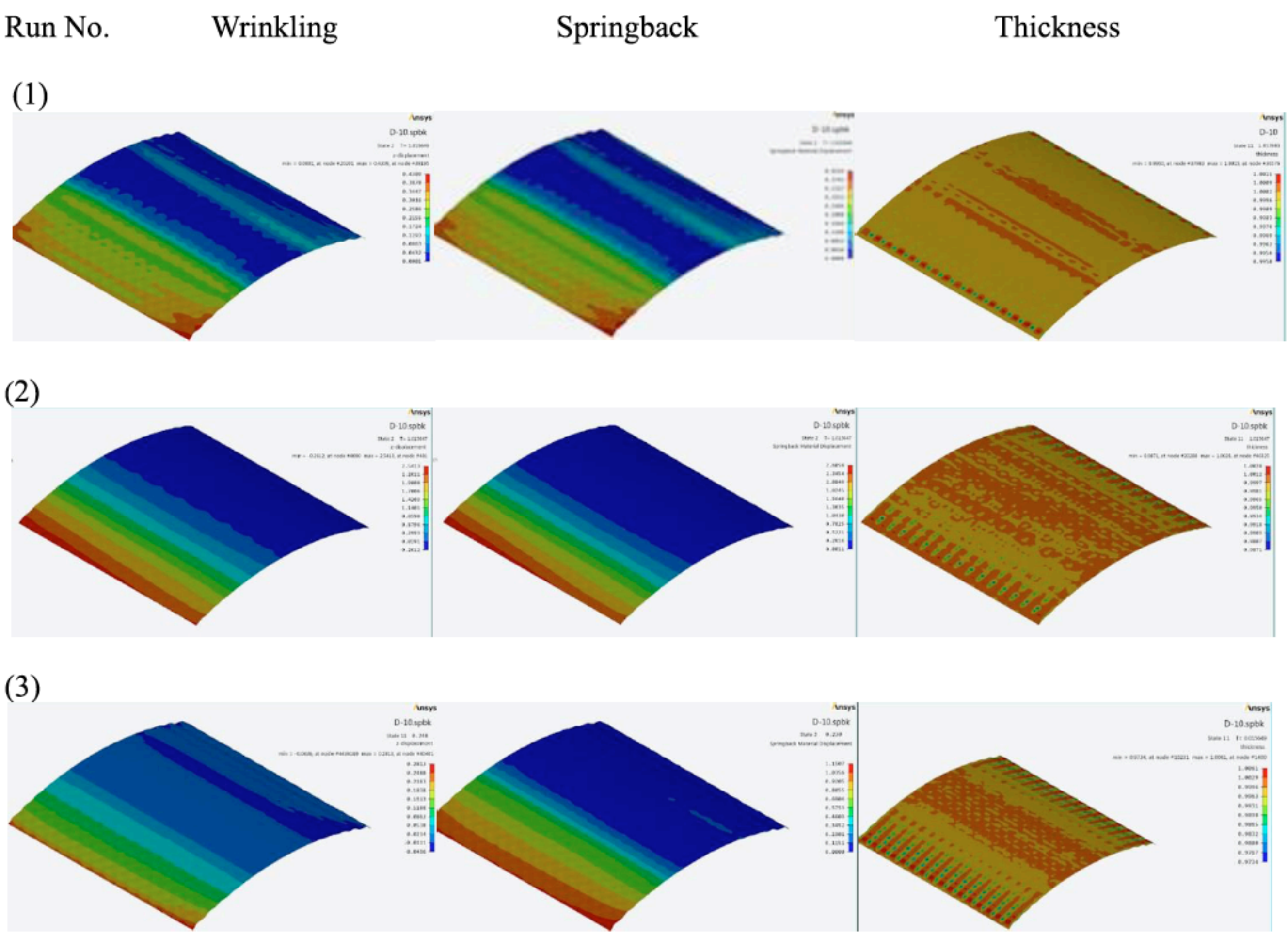

APPENDIX

Run No. Wrinkling Springback Thickness

(4)

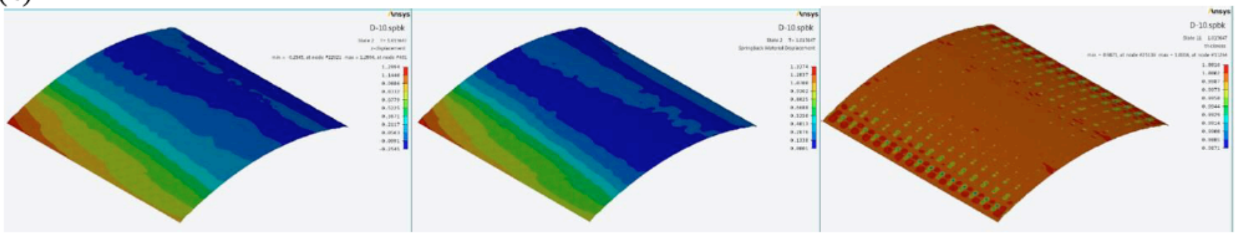

(5)

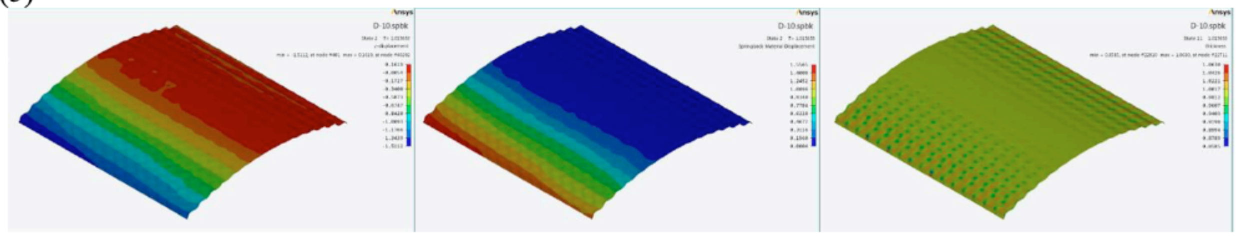

(6)

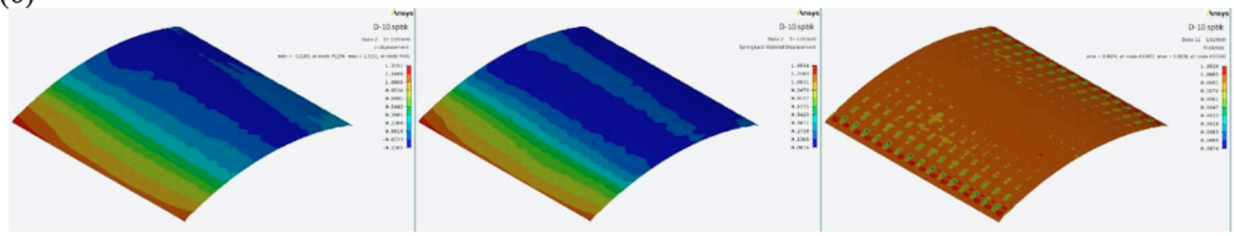

(7)

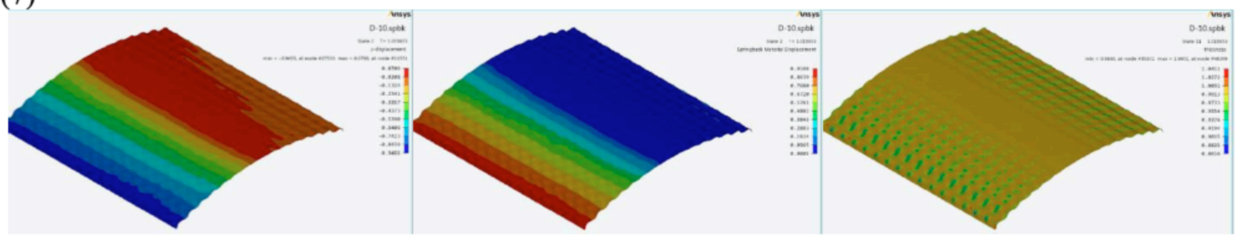

(8)

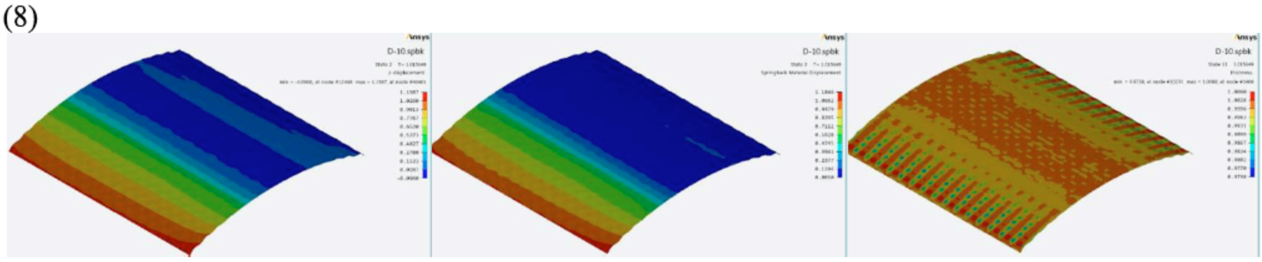

(9)

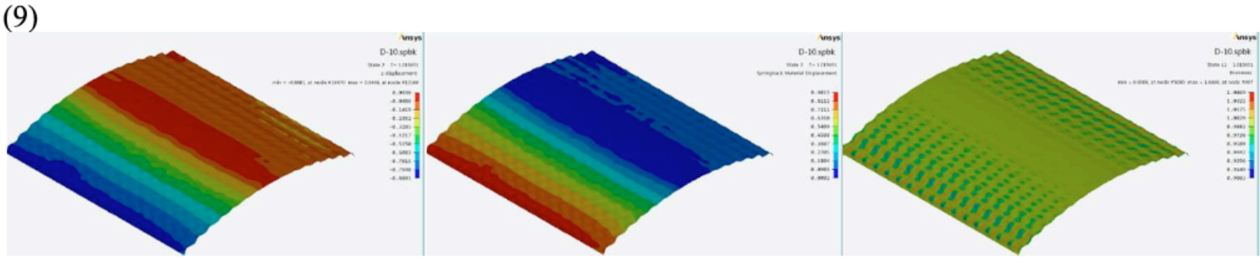

APPENDIX

Run No. Wrinkling Springback Thickness

(10)

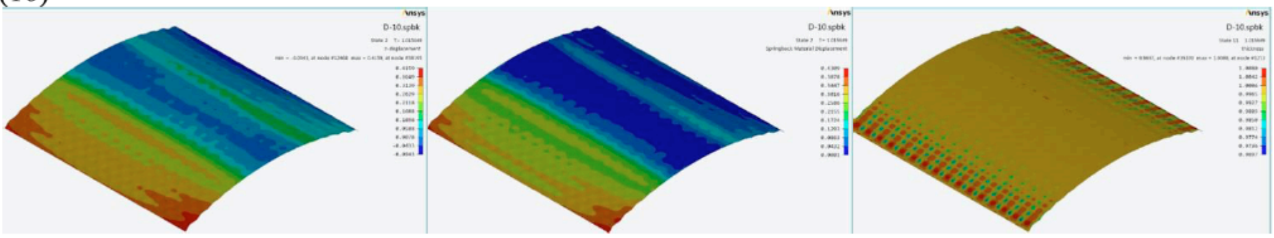

(11)

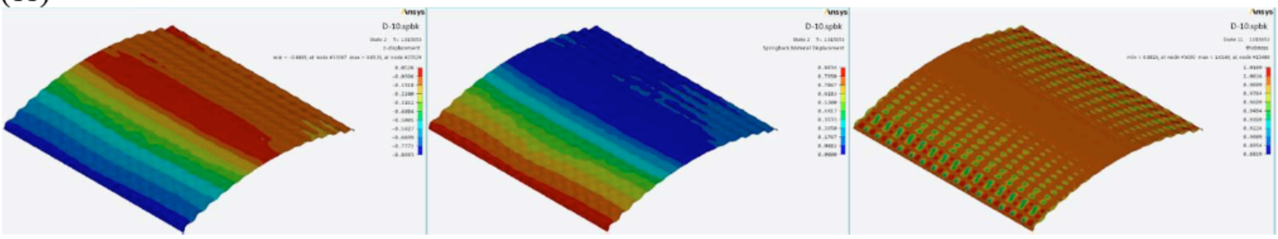

(12)

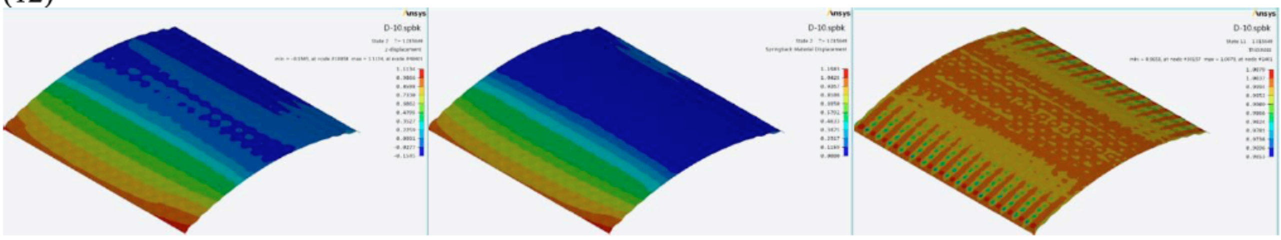

(13)

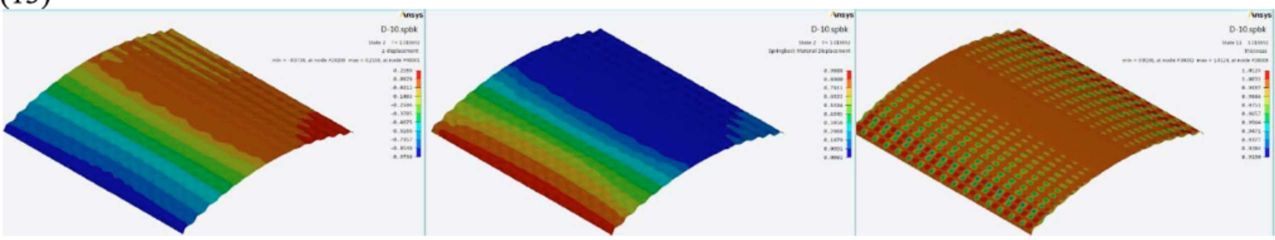

(14)

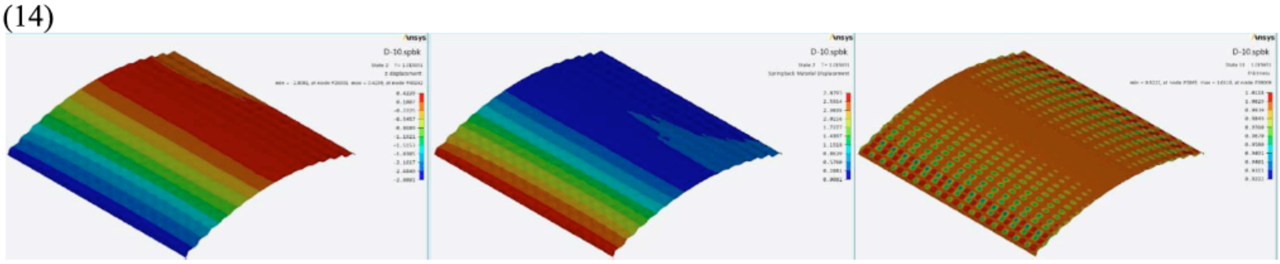

(15)

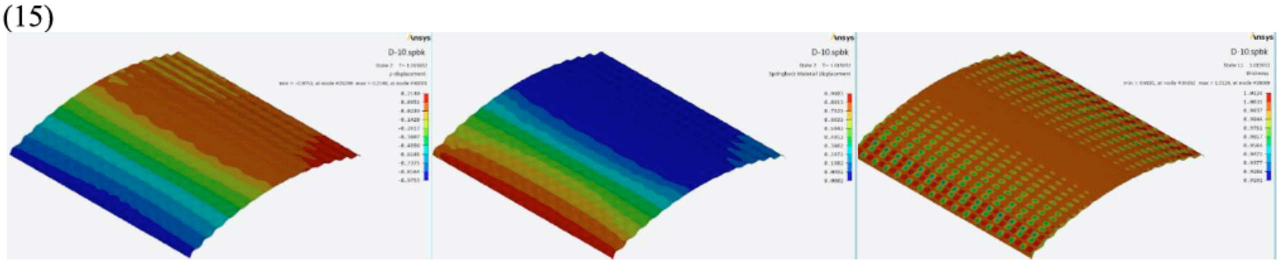

APPENDIX

Run No. Wrinkling Springback Thickness

(16)

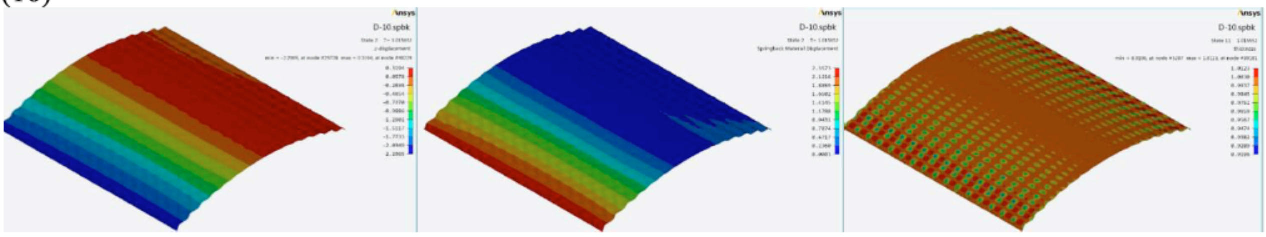

(17)

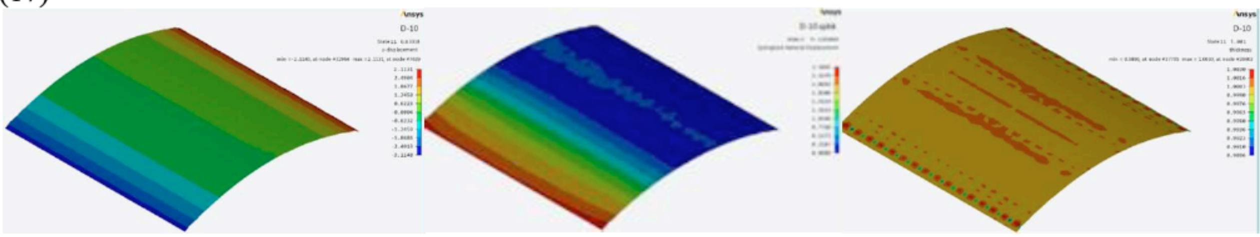

(18)

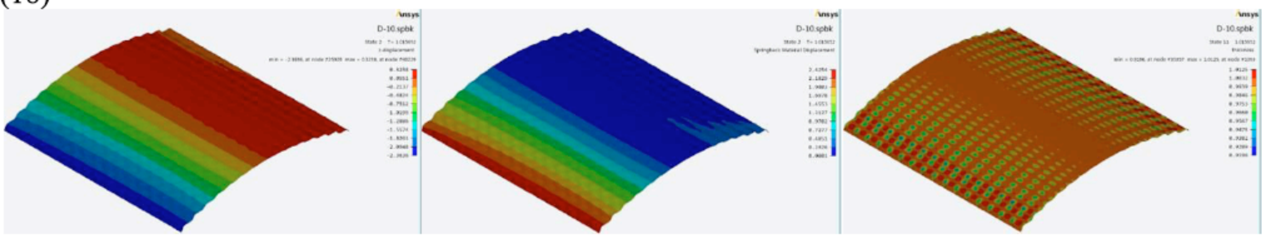

(19)

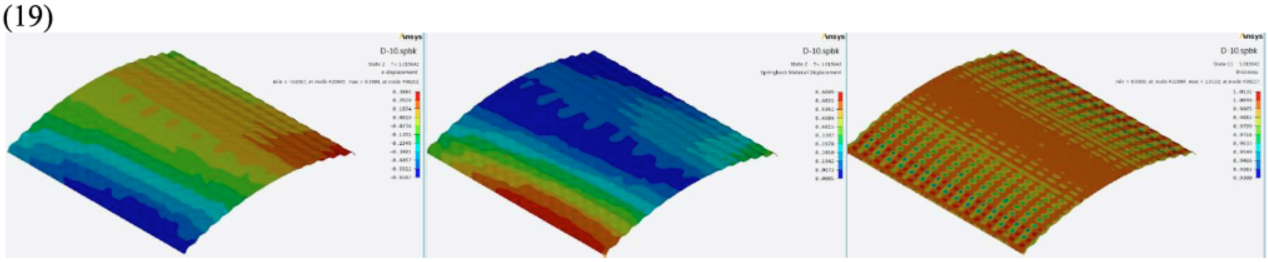

(20)

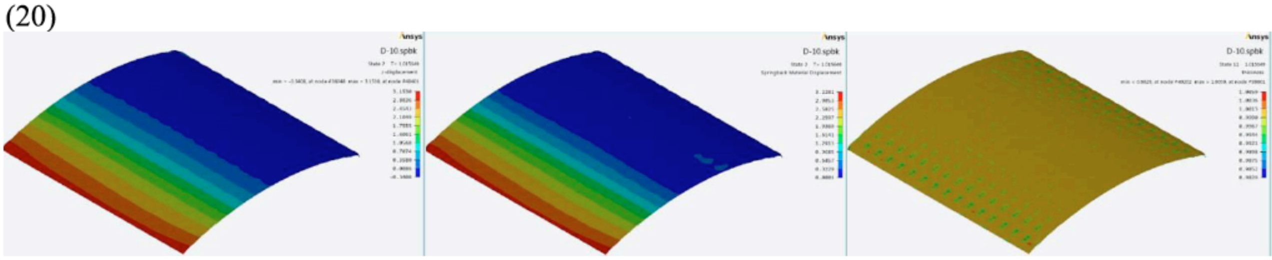

(21)

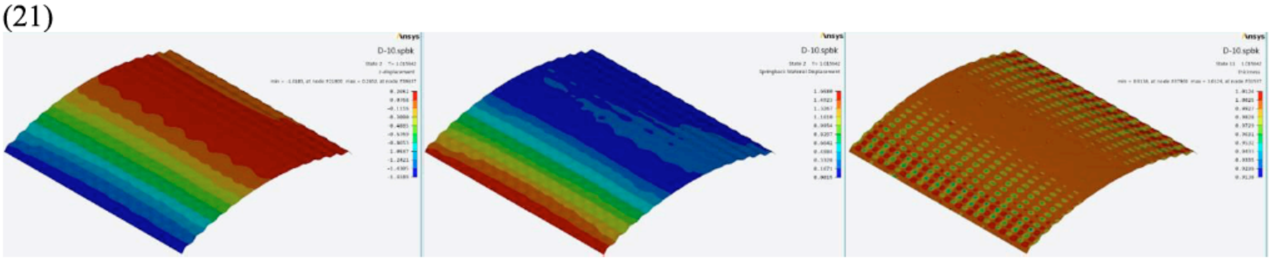

APPENDIX

Run No. Wrinkling Springback Thickness

(22)

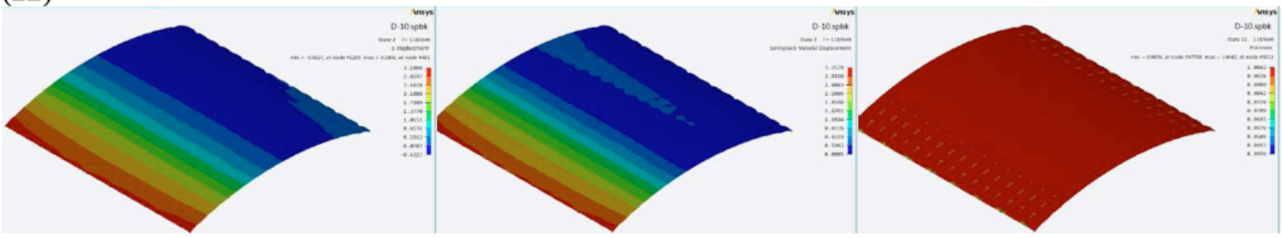

(23)

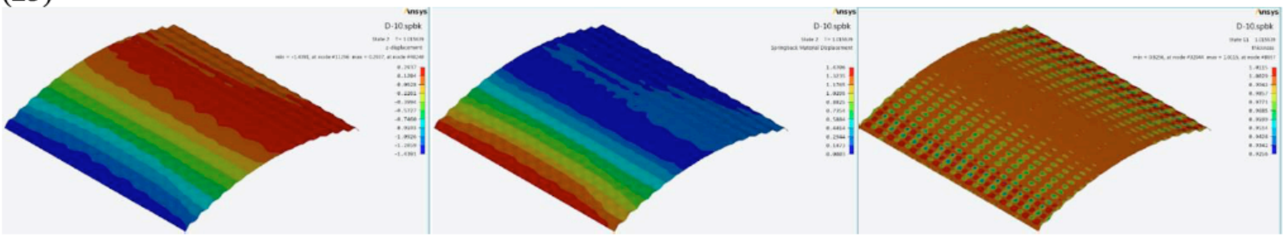

(24)

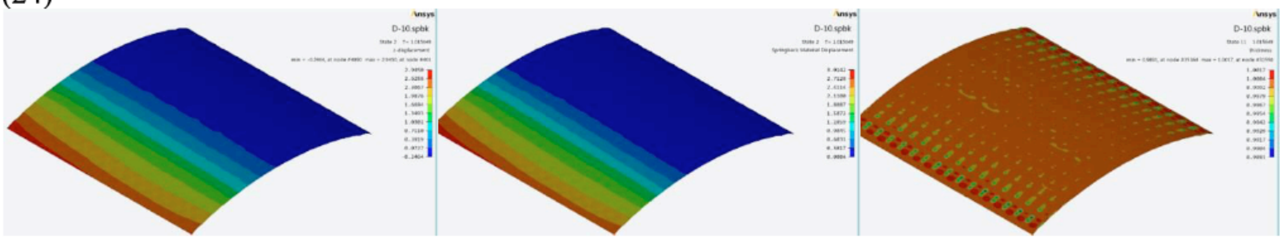

(25)

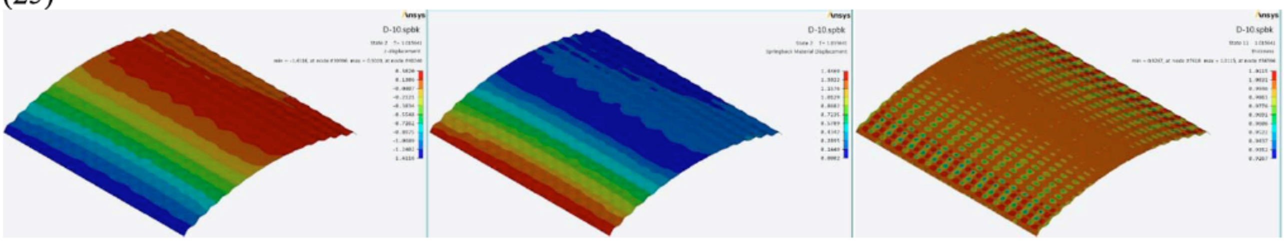

(26)

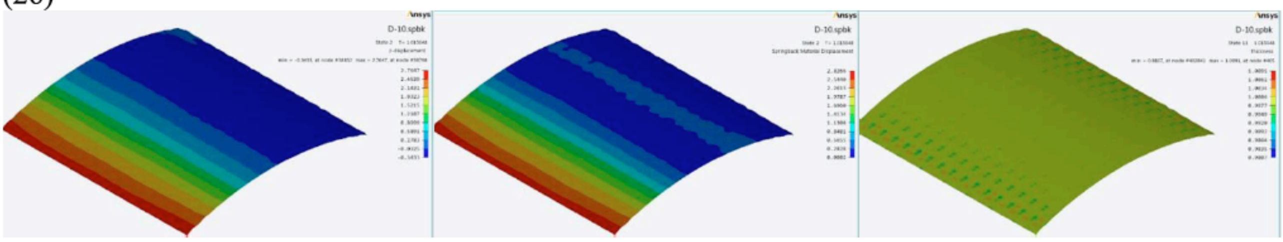

(27)

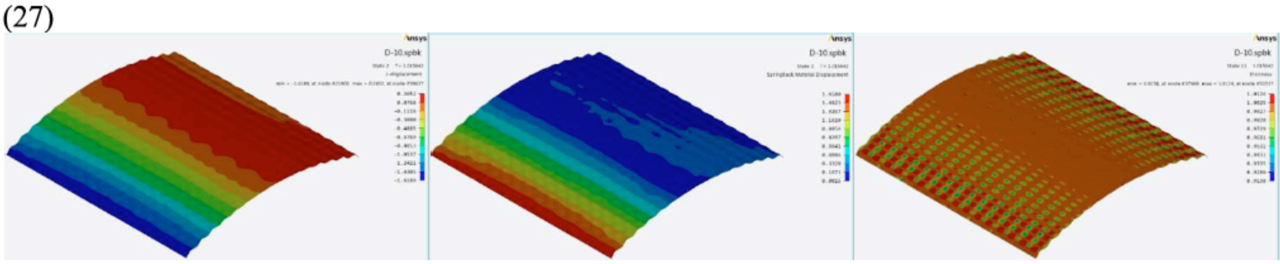

APPENDIX

Run No.	Wrinkling	Springback	Thickness

(28)

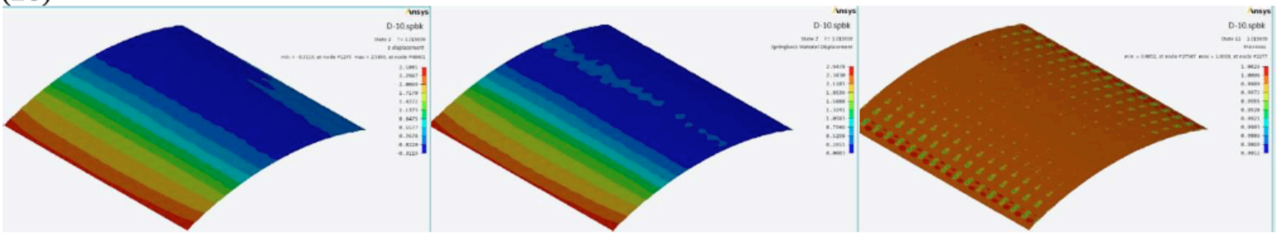

(29)

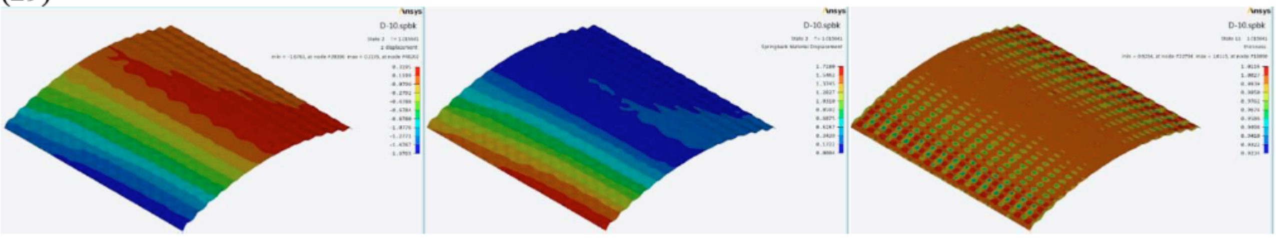

(30)

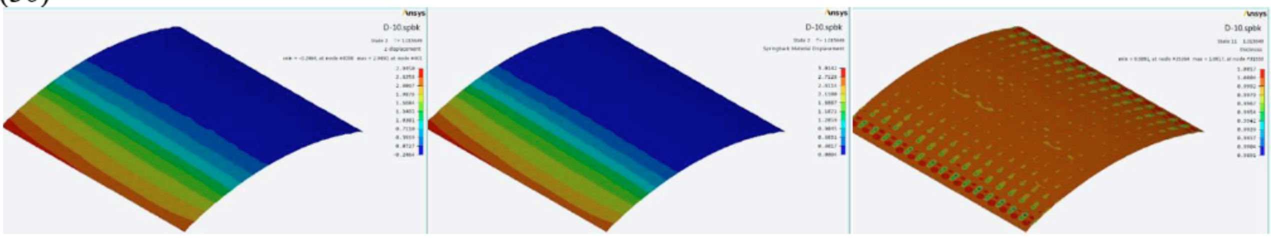

(31)

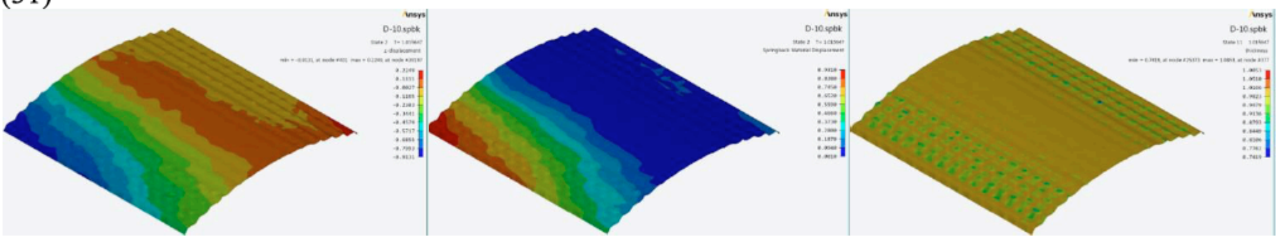

(32)

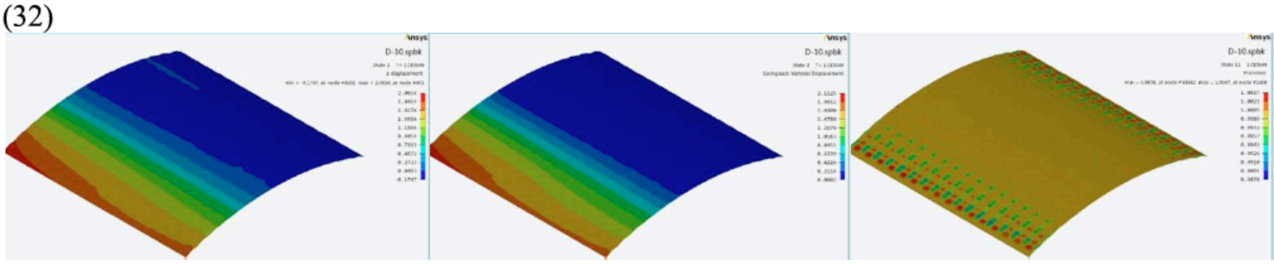

(33)

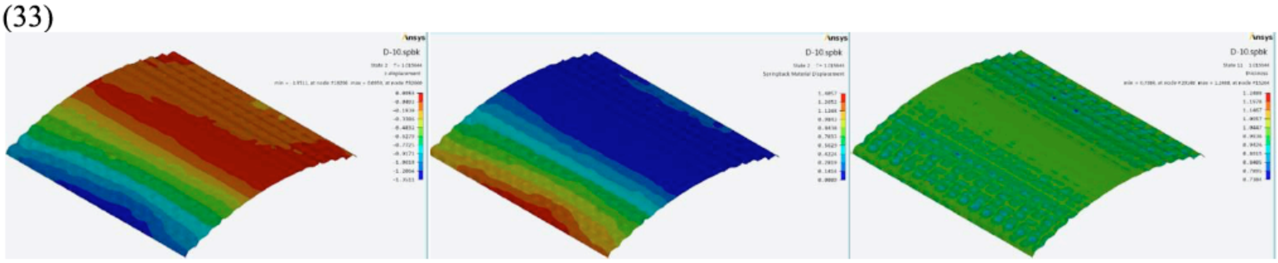

APPENDIX

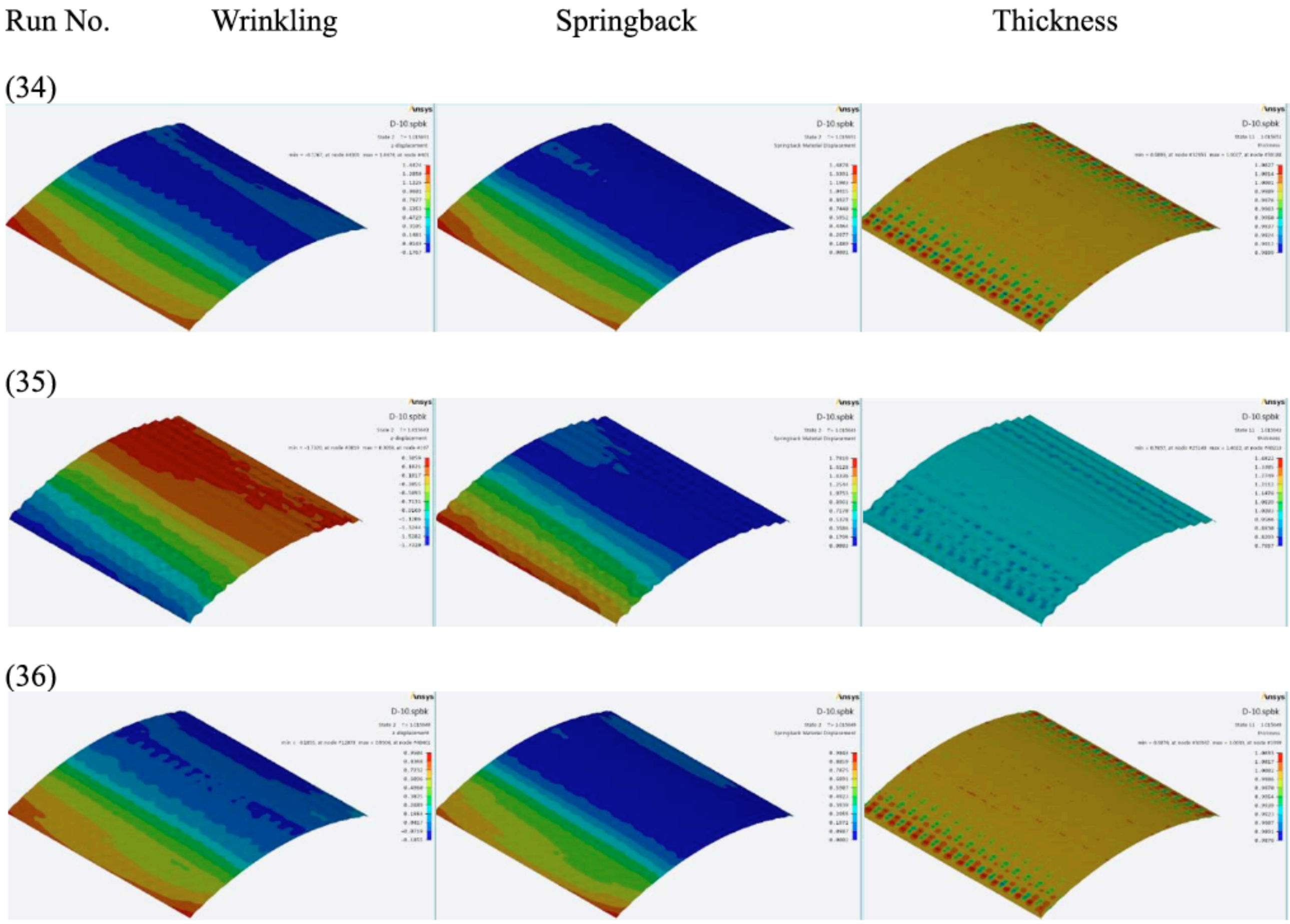

REFERENCES

[1] He X, Welo T, Ma J. In-process monitoring strategies and methods in metal forming: A selective review. Journal of Manufacturing Processes. 2025; 138: 100-28. https://doi.org/10.1016/j.jmapro.2025.02.011

[2] Tolipov A, Elghawail A, Abosaf M, Pham D, Hassanin H, Essa K. Multipoint forming using mesh-type elastic cushion: modelling and experimentation. The International Journal of Advanced Manufacturing Technology. 2019; 103(5): 2079-90. https://doi.org/10.1007/s00170-019-03635-z

[3] Al-Ghuraibawi A, Abed AH, Mansor KK. Simulation and Experimental Approach for Metal Forming with a Multi-Point Die. Salud, Ciencia y Tecnología - Serie de Conferencias. 2024; 3: 855. https://doi.org/10.56294/sctconf2024855

[4] Selmi N, Belhadjsalah H, editors. .Flexible multipoint hydroforming using metallic sheet medium. Second Tunisian Congress of Mechanics; 2012. Tunisia2012.

[5] Zareh-Desari B, Davoodi B, Vedaei-Sabegh A. Investigation of deep drawing concept of multi-point forming process in terms of prevalent defects. International Journal of Material Forming. 2017; 10(2): 193-203. https://doi.org/10.1007/s12289-015-1268-1

[6] Shen W, Yan R, Lin Y, Li P. Evaluation of residual stress for multi-point repeated forming technology. Ships and Offshore Structures. 2020; 15(8): 815-28. https://doi.org/10.1080/17445302.2019.1686228

[7] Maier P, Ruback C, Rappsilber E, Schellhorn H, editors. Multi-point forming of Al sheets of various thickness using elastic cushion. 23rd International Symposium "Research-Education-Technology"; 2017; Stralsund.

[8] Peng H, Li M, Liu C, Cao J. Study of multi-point forming for polycarbonate sheet. The International Journal of Advanced Manufacturing Technology. 2013; 67(9): 2811-7. https://doi.org/10.1007/s00170-012-4694-y

[9] Li X, Hu S. Research Progress of Springback in Multi-Point Forming of Sheet Metal. Journal of Physics: Conference Series. 2021; 2101(1): 012006. https://doi.org/10.1088/1742-6596/2101/1/012006

[10] Tolipov A, Hassanin H, El-Sayed MA, Eldessouky HM, Alsaleh NA, Alfozan AK, Essa K, Ahmadein M. Multipoint Forming Using Hole-Type Rubber Punch. metals. 2022; 12(3): 491. https://doi.org/10.3390/met12030491

[11] Beglarzadeh B, Davoodi B. Numerical simulation and experimental examination of forming defects in multi-point deep drawing process. Mechanics. 2016; 22. https://doi.org/10.5755/j01.mech.22.3.15252

[12] Li X, Hu S. Numerical Simulation and Experimental Research on Multi-Point Forming of Aluminum Alloy Sheets Based on Ultrasonic Vibration. Mathematical Problems in Engineering. 2022; 2022(1): 7688376. https://doi.org/10.1155/2022/7688376

[13] Viorel P, Cekan P, Banu M, Epureanu A, Nicoara D. Simulation of the Combined Reconfigurable Multipoint Forming and Rubber Forming: 12th International Conferecne on Metal Forming; 2008. 549-54 p.

[14] Elghawail A, Essa K, Abosaf M, Tolipov A, Su S, Pham D. Low-cost metal-forming process using an elastic punch and a reconfigurable multi-pin die. International Journal of Material

Forming. 2019; 12(3): 391-401.
https://doi.org/10.1007/s12289-018-1423-6

[15] Al-Ghuraibawi A, Abed A, Mansor K. Numerical Simulation of Forming a 3D Shape by a Multi-Point Die. Salud, Ciencia y Tecnología - Serie de Conferencias. 2024; 3: 848.
https://doi.org/10.56294/sctconf2024848

[16] Tolipov AA, Elghawail A, Shushing S, Pham D, Essa K. Experimental research and numerical optimisation of multi-point sheet metal forming implementation using a solid elastic cushion system. Journal of Physics: Conference Series. 2017; 896(1): 012120.
https://doi.org/10.1088/1742-6596/896/1/012120

[17] Chiaia P, Cinefra M, Carrera E. Curvilinear 2|3D finite elements for the analysis of shells with arbitrary curvature and variable thickness. Computers & Structures. 2025; 317: 107911.
https://doi.org/10.1016/j.compstruc.2025.107911

[18] Majidabad MA, Hashemi R, Akbari H. Effects of layer arrangement, pin size, polyurethane thickness, and polyurethane hardness on forming limits of Al/Cu bimetallic sheets through multi-point forming process. Journal of Materials Research and Technology. 2025; 34: 396-407.
https://doi.org/10.1016/j.jmrt.2024.12.013

[19] Yang S, Wen Y, Liang C, Li Y. Study on the Influence of Isotropic Simplification in Flexible Multi-Point Stretch-Bending Forming with Roller Dies. metals. 2025; 15(9): 1036.
https://doi.org/10.3390/met15091036

[20] Hao S, Wang W, Wang X, Yan J, Shi H, Cheng X, Ding R, Han Q. Fabrication and Surface Quality of Thermoformed Composite Saddles Using Hexagonal-Patterned Multi-Point Tooling. Eng. 2026; 7(2): 69.
https://doi.org/10.3390/eng7020069

[21] Ding R, Cheng X, Cao L, Hao S, Wang X, Wang W, Yan J, Shi H, Sun J, Li Y, Han Q. Wrinkle suppression in high-strength steel curved components through sequential loading in multi-point forming with enhanced normal compressive stress. Journal of Materials Processing Technology. 2026; 350: 119262.
https://doi.org/10.1016/j.jmatprotec.2026.119262

[22] Abosaf M, Essa K, Alghawail A, Tolipov A, Su S, Pham D. Optimisation of multi-point forming process parameters. The International Journal of Advanced Manufacturing Technology. 2017; 92(5): 1849-59.
https://doi.org/10.1007/s00170-017-0155-y

[23] Viorel Păunoiu CM, Virgil Teodor & Eugen Găvan. Numerical Analysis of Multipoint Forming Process. International Journal of Modern Manufacturing Technologies. 2011; III(2): 85-90.

[24] Moheen M, Abdel-Wahab A, Hassanin H, Essa K. Reconfigurable Multipoint Forming Using Waffle-Type Elastic Cushion and Variable Loading Profile. Materials. 2020; 13(20): 4506.
https://doi.org/10.3390/ma13204506

[25] Karakaya Ç, Ekşi S. Springback Behavior of AA 7075-T6 Alloy in V-Shaped Bending. Applied Sciences. 2025; 15: 5509.
https://doi.org/10.3390/app15105509

[26] Jeswiet J, Micari F, Hirt G, Bramley A, Duflou J, Allwood J. Asymmetric Single Point Incremental Forming of Sheet Metal. CIRP Annals. 2005; 54(2): 88-114.
https://doi.org/10.1016/S0007-8506(07)60021-3

[27] Cai Z-Y, Wang S-H, Li M-Z. Numerical investigation of multi-point forming process for sheet metal: wrinkling, dimpling and springback. The International Journal of Advanced Manufacturing Technology. 2008; 37(9): 927-36.
https://doi.org/10.1007/s00170-007-1045-5

[28] Wagoner R, Lim H, Lee M-G. Advanced Issues in springback. International Journal of Plasticity. 2013; 45: 3-20.
https://doi.org/10.1016/j.ijplas.2012.08.006

[29] Ambrogio G, Filice L, Micari F. A force measuring based strategy for failure prevention in incremental forming. Journal of Materials Processing Technology. 2006; 177(1): 413-6.
https://doi.org/10.1016/j.jmatprotec.2006.04.076

[30] Wen Y, Liang J, Li Y, Liang C. Springback Control of Profile by Multi-Point Stretch-Bending and Torsion Automatic Forming Based on FE-BPNN. metals. 2025; 15(5): 544.
https://doi.org/10.3390/met15050544

[31] Zhao X, Ou H. A new flexible multi-point incremental sheet forming process with multi-layer sheets. Journal of Materials Processing Technology. 2023; 322: 118214.
https://doi.org/10.1016/j.jmatprotec.2023.118214

[32] Allwood J. M. KGPF, Duflou J. A structured search for applications of the incremental sheet-forming process by product segmentation. Proceedings of the Institution of Mechanical Engineers. 2005; 219(2): 239-44.
https://doi.org/10.1243/095440505X8145

https://doi.org/10.31875/2409-9848.2026.13.05